Journal of Wind Engineering & Industrial Aerodynamics 224 (2022) 104978

Contents lists available at ScienceDirect

Journal of Wind Engineering & Industrial Aerodynamics

journal homepage: www.elsevier.com/locate/jweia

Maximum dynamic response of linear elastic SDOF systems based on an evolutionary spectral model for thunderstorm outflows

Luca Roncallo [a,*], Giovanni Solari [a], Giuseppe Muscolino [b], Federica Tubino [a]

[a] Department of Civil, Chemical and Environmental Engineering (DICCA), Polytechnic School, University of Genoa, Via Montallegro 1, 16145, Genoa, Italy
[b] Department of Engineering, University of Messina, Villaggio S. Agata, 98166, Messina, Italy

ARTICLE INFO

Keywords:
Equivalent parameters technique
Evolutionary power spectral density
Nonstationary dynamic response
Nonstationary peak factor
Response spectrum technique
Thunderstorm outflows
Wind engineering

ABSTRACT

The study aims to estimate the maximum dynamic response of linear elastic SDOF systems subjected to thunderstorm outflows. Starting from a recently developed Evolutionary Power Spectral Density (EPSD) model for the wind velocity, the dynamic response is decomposed into a time-varying mean and a non-stationary random fluctuation. The EPSD and the Non-Geometrical Spectral Moments (NGSMs) of the random fluctuation are derived both accounting and neglecting the transient dynamics due to the modulating function of the load. The mean value of the maximum nonstationary fluctuating component of the response is estimated based on the definition of an equivalent stationary process following an approach proposed in the literature. In order to mitigate the overestimations of the maximum dynamic response due to the Poisson approximation, analogously to the formulation developed by Der Kiureghian for withe noise excitation, an equivalent expected frequency is introduced for thunderstorm excitation. Finally, the maximum dynamic response to thunderstorms is estimated as the sum of the maximum mean and fluctuating parts and a numerical validation of the results against real recorded thunderstorms is provided, highlighting the reliability of adding up the mean and fluctuating contributions and the advantages and limits of neglecting the transient dynamics.

1. Introduction

Wind and earthquakes constitute the main natural hazards that strike the natural and built environment, causing damages and losses in our societies. In this regard, the modelling and prediction of their action and the evaluation of their impact on structures represent one of the most important goals for civil engineers to design safe and cost-efficient structures.

Wind can occur around the world in the form of tropical and extra-tropical cyclones, tornadoes, downslope winds and thunderstorms. In particular, the occurrence of extra-tropical cyclones and thunderstorms affects the whole planet, dominating the European wind climate.

For what concerns extra-tropical cyclones, the theory and models for the wind velocity and the wind-excited structural response are well-established in design codes (Davenport, 1961, 1964, 1967; Solari, 1982, 1993a, 1993b, 2019). On the other hand, despite the great amount of research carried out in the last decades, the representation of wind velocity associated to thunderstorm outflows (e.g. Chen and Letchford, 2005; Holmes et al., 2008; Lombardo et al., 2014; Lombardo and Zickar, 2019; McConville et al., 2009) and the calculation of the related structural dynamic response is still an open issue and a crucial topic in wind engineering. Indeed, thunderstorms are mesoscale phenomena with extension of few kilometres and short duration, which makes them difficult to be detected by one single anemometer. Moreover, the nonstationary nature of the wind field generated by thunderstorms makes most of the theory and models developed for extra-tropical cyclones unsuitable and, to date, it has prevented the development of robust models for rapid engineering calculations shared by the scientific community. In this regard, different methods and advanced techniques have been proposed in the literature, including time-domain solutions, response spectrum technique and time-frequency analyses.

Choi and Hidayat (2002), with the aim to generalize the gust factor technique, studied the dynamic response of Single Degree Of freedom (SDOF) systems subjected to thunderstorm wind loading in time domain, expressing the maximum as the sum of the maximum of the mean part of the response and the maximum of the standard deviation of its fluctuating part multiplied by a peak factor. Chen and Letchford (2004a, 2004b) studied a deterministic-stochastic hybrid model of thunderstorms and they expressed the maximum dynamic response of a real structure as a function of the maximum dynamic magnification

* Corresponding author.
E-mail address: luca.roncallo@edu.unige.it (L. Roncallo).

https://doi.org/10.1016/j.jweia.2022.104978
Received 24 December 2021; Received in revised form 19 February 2022; Accepted 16 March 2022

factor. Similarly, Holmes et al. (2005) studied the maximum dynamic response of a SDOF system to a sample of a real thunderstorm event through a response factor, while Chay and Albermani (2005) analysed the dynamic response of a SDOF system to a simulated downburst.

Starting from time domain analysis of real recorded thunderstorms, the thunderstorm response spectrum technique (TRST) was developed by Solari et al. (2015b) for linear elastic SDOF systems, aiming to provide a robust tool to be used by engineers from an operative perspective. Then, the TRST has been extended to MDOF systems through the equivalent wind spectrum technique (Solari, 1988, 2016).

Time-frequency analyses include advanced techniques such as wavelets and Evolutionary Power Spectral Density (EPSD) models. The wavelet technique was employed by Le and Caracoglia (2017, 2015) to study the dynamic response of a tall building subjected to the downburst wind load, developing a computer based model for its calculation starting from a digitally simulated thunderstorm. Successively, the dynamic response of a tall building to the downburst wind loading was also investigated by means of the Fokker-Planck Equation with a parametric study (Caracoglia, 2017). EPSD models for thunderstorms have been adopted by different researchers. Chen (2008) studied the alongwind response of a tall building to nonstationary winds, deriving the EPSD of the response both accounting and neglecting the effect of the transient dynamics on the standard deviation. Kwon and Kareem (2009), based on an ideal EPSD model of wind velocity, proposed a gust front factor approach able to encapsulate the features of the gust-front wind effects. They recently revisited the framework providing closed-form solutions based on the assumption of long-pulse duration (Kwon and Kareem, 2019). The effects of the time-varying mean and standard deviation of the wind velocity on the dynamic response of tall buildings was investigated by Huang et al. (2013) in time domain, starting from the numerical simulation of time-histories compatible with an EPSD estimated from a full-scale wind speed record. Peng et al. (2018), based on the analysis of two thunderstorm records, introduced a model of a time-varying coherence function for downburst winds and adopted it for the estimate of the alongwind dynamic response of ideal tall buildings. More recently, Kareem et al. (2019) proposed a generalization of the original Davenport's wind loading chain (Davenport, 1967) in time-frequency domain for nonstationary winds, employing both wavelets and the EPSD to derive the dynamic response of Multi Degree Of Freedom (MDOF) systems.

Nevertheless, even though different models and methods accomplished with robust theoretical bases have been proposed in the literature, a unified and reliable analytical model for the assessment of the maximum dynamic response to thunderstorms coherent with the techniques commonly adopted in wind engineering (i.e. gust factor) is not yet available. In most cases, applications to a single structure or specific case studies have been proposed (Chen and Letchford, 2004a, 2004b; Choi and Hidayat, 2002). Moreover, most of the analyses and models are either based on few records of thunderstorm wind velocity, on simulations of downburst starting from estimated EPSD or even only theoretically conceptualized (Holmes et al., 2005; Huang et al., 2013, 2015; Huang and Chen, 2009; Kareem et al., 2019; Kwon and Kareem, 2009, 2019; Le and Caracoglia, 2017; Peng et al., 2018). This is a major shortcoming since the time-histories of thunderstorm outflows can be significantly different from one another and hence to rely on few or even only one record for their modelling can be a rather questionable approach.

In this context, the great seaport monitoring network of anemometers in the Tyrrenian sea realized by the Department of Civil, Chemical and Environmental Engineering (DICCA) of the University of Genoa, in the framework of the European projects "Wind and Ports" and "Wind, Ports and Sea" (Repetto et al., 2017, 2018; Solari et al., 2012), includes 28 ultrasonic anemometers which collected more than 270 nonstationary events in the last seven years. This wide database allowed the GS-Windyn Research Group (www.gs-windyn.com) to carry out a considerable amount of research both on the characteristics of thunderstorm outflows (Burlando et al., 2017, 2018; De Gaetano et al., 2014; Solari et al., 2015a; Tubino and Solari, 2020; Zhang et al., 2017, 2018, 2019) and on the related dynamic response of SDOF and MDOF systems (Solari, 2016; Solari et al., 2015b, 2017; Solari and De Gaetano, 2018), laying the foundations to the research project THUNDERR: Detection, simulation, modelling and loading of thunderstorm outflows to design wind-safer and cost efficient structures. Starting from the available large database of thunderstorm records, an EPSD model of thunderstorm outflows consistent with full-scale thunderstorm records has been developed (Roncallo and Solari, 2019, 2020).

The present paper aims to study the possibility of extending the traditional approach of the gust factor technique to the estimate of the maximum dynamic response of linear SDOF systems to thunderstorm outflows starting from the consistent EPSD model for the wind velocity developed (Roncallo and Solari, 2019, 2020). The mean value of the maximum dynamic response should be estimated from its pdf defined on the basis of the up-crossing theory of nonstationary processes, taking into account the variation in time of the mean part of the response and of the standard deviation (Hu and Xu, 2014; Huang et al., 2013; Kareem et al., 2019). However, this procedure has the shortcoming of being unsuitable to be applied within an operative context and hence to be declined in codes for rapid engineering calculations. Hence, an alternative approach to the direct calculation of the mean value of the maximum response is investigated, able to adapt the gust factor formulation for synoptic winds to thunderstorm outflows. Coherently with the proposal by Kwon and Kareem (2019, 2013, 2009), the approach is based on a technique proposed in literature for the estimate of the maximum of a nonstationary process with zero-mean, introducing suitable equivalent parameters (Michaelov et al., 2001), here called Equivalent Parameters Technique (EPT). The application of the EPT for the estimate of the maximum of the fluctuating part of the response allows to express the global maximum in the same form as for synoptic winds. However, its extension to the estimate of the maximum response to thunderstorms is a delicate aspect, since the dynamic response is not zero-mean and the maxima of the mean and fluctuating parts need to be recombined.

In this study, the EPT is adopted to estimate the mean value of the maximum of the fluctuating part of the dynamic response starting from an EPSD model for the thunderstorm wind velocity consistent with a large number of real thunderstorm records. Analyses are carried out on a wide range of linear SDOF systems with variable fundamental frequencies and damping ratios both accounting and neglecting the effects produced by the transient dynamics. The mean value of the maximum response is then derived as the summation of the maxima of the mean and of the fluctuating part of the response. Finally, the approach is validated comparing the EPSD-based maximum response with the mean value of the maximum dynamic response to 129 real thunderstorms recorded at full scale, estimated numerically through step-by-step time domain analyses (Roncallo and Solari, 2020). The advantage and limits of neglecting the transient dynamics and the reliability of the assumption of contemporaneity between the maxima of the mean and fluctuating part of the response are discussed.

The paper is articulated as follows: Section 2 provides a brief overview on the EPSD model adopted for the wind velocity and the derivation of the wind load; Section 3 reports the derivation of the dynamic response outlining two different approaches: the first one, named Rigorous method, derives the dynamic response directly through the NGSMs, while the second approach, named Simplified method, assumes the modulating function of the loading as slowly-varying with respect to the fundamental period of the structure. Section 4 is dedicated to the statistical characterization of the maximum of the fluctuating part of the response, introducing an equivalent stationary process to define the peak factor both for the Rigorous and Simplified method; Section 5 introduces an effective zero-crossing rate based on the method proposed by Der Kiureghian with reference to a white noise excitation; Section 6 deals with the combination of the maximum of the mean and fluctuating

parts of the response and the validation against the maximum response numerically derived from real recorded events. Finally Section 7 outlines the conclusions and the prospects of the study.

2. EPSD model for the wind load

Let us consider a point-like structure, immersed in a wind field generated by a thunderstorm outflow characterized by the wind velocity $v(t)$, being $t \in \left[-\frac{T_{max}}{2}, \frac{T_{max}}{2}\right]$ the time and T_{max} the temporal interval in which the thunderstorm outflow occurs, namely $T_{max} = 600$ s (Roncallo and Solari, 2020; Zhang et al., 2017). Neglecting the role of the partial wind correlation together with the variation of the velocity along the structure and its change of direction, the alongwind force is defined as:

$$f(t) = \frac{1}{2}\rho v^2(t) A c_D \tag{1}$$

where ρ is the air density, A the area exposed to the wind and c_D the drag coefficient. It is worth to point out that, in general, the drag coefficient, being a function of the angle of attack, may be affected by the change of direction of the wind velocity during the thunderstorm. However, in this study, the effect of the variation of the wind direction is neglected and c_D is assumed as constant. Following "Method B″ described in Roncallo and Solari (2020), the velocity $v(t)$ is modelled as a uniformly modulated process as follows:

$$v(t) = \bar{v}_{max}\gamma(t)[1 + \bar{I}_v \tilde{v}'(t)] \tag{2}$$

with $\bar{v}_{max}$ and $\gamma(t)$, respectively, the maximum value and the deterministic modulating function of the slowly-varying mean wind velocity, $\bar{I}_v$ the mean value of the turbulence intensity and $\tilde{v}'(t)$ the so-called reduced turbulent fluctuation, dealt with as a zero-mean stationary Gaussian random process with unitary standard deviation. It is worth to point out that in Eq. (2) it is implicitly assumed that the turbulence intensity is constant and hence the mean wind velocity and turbulent fluctuations are modulated by the same function $\gamma(t)$. This hypothesis, allowing a simpler treatment of the wind load, can lead in some cases to slight overestimations of the dynamic response (Roncallo and Solari, 2020). Substituting Eq. (2) into Eq. (1) and invoking the hypothesis of small turbulence, the alongwind force takes the following form:

$$f(t) = C\bar{v}^2_{max}\gamma^2(t)[1 + 2\bar{I}_v \tilde{v}'(t)] \tag{3}$$

having defined $C = 1/2\rho A c_D$. The alongwind force in Eq. (3) can be decomposed as follows:

$$f(t) = \bar{f}(t) + f'(t) \tag{4}$$

where $\bar{f}(t)$ and $f'(t)$ are, respectively, the mean and fluctuating part of the loading, given by:

$$\bar{f}(t) = C\bar{v}^2_{max}\gamma^2(t) \tag{5}$$

$$f'(t) = 2C\bar{I}_v\bar{v}^2_{max}\tilde{f}'(t) \tag{6}$$

where $\tilde{f}'(t)$ is the reduced fluctuating part of the loading:

$$\tilde{f}'(t) = \gamma^2(t)\tilde{v}'(t) \tag{7}$$

Thus, the fluctuating part of the alongwind force (Eq. (6)), as well as its reduced counterpart (Eq. (7)) are uniformly modulated random processes, making the derivation of their one-sided Evolutionary Power Spectral Density (EPSD) straightforward (Lin and Cai, 1995; Priestley, 1965):

$$S_{f'}(n,t) = \left(2C\bar{I}_v\bar{v}^2_{max}\right)^2 \underset{f}{S}(n,t) \tag{8}$$

$$\underset{f}{S}(n,t) = \gamma^4(t)\underset{v}{S}(n) \tag{9}$$

where n is the frequency and $\underset{v}{S}(n)$ the one-sided PSD of the reduced turbulent fluctuations. For the analyses carried out in the study, the function $\gamma(t)$ is defined as follows (Roncallo and Solari, 2020):

$$\gamma(t) = \frac{1 - \gamma^*}{\left[1 + \left(\frac{t}{T_\gamma}\right)^2\right]^{\frac{1}{2}}} + \gamma^* \tag{10}$$

where the parameters γ^* and T_γ are, respectively, a measure of the intensity of the background mean wind velocity and a measure of the duration of the thunderstorm peak. In the literature, different models were proposed to describe the modulating function of the slowly-varying mean wind velocity (e.g. Abd-Elaal et al., 2013; Chay et al., 2006; Kwon and Kareem, 2009; Ponte and Riera, 2010). The model in Eq. (10) furnishes the best representation of the trend of the slowly-varying mean wind velocity extracted from 129 full-scale thunderstorm records (Roncallo and Solari, 2020). It should be pointed out that the parameters γ^* and T_γ vary from one thunderstorm to one another. In the present study, the parameters $\gamma^* = 0.45$ and $T_\gamma = 26.45$ s are assumed, providing the best fit of the mean trend of the sample functions of the full-scale slowly-varying mean wind velocities (Roncallo and Solari, 2020).

The one-sided PSD of the reduced turbulent fluctuations is modelled by means of the spectral model introduced by Solari and Piccardo (2001):

$$\underset{v}{S}(n) = \frac{1}{n}\frac{6.868 n L_v/\bar{v}_{max}}{[1 + 10.302 n L_v/\bar{v}_{max}]^{5/3}} \tag{11}$$

assuming $L_v/\bar{v}_{max} = 1.72$ s as evaluated from the thunderstorm time histories in (Roncallo and Solari, 2020).

As an example, Fig. 1 plots the one-sided EPSD of the reduced fluctuating part of the load $\underset{f}{S}$ as a function of the reduced frequency $\tilde{n} = nL_v/\bar{v}_{max}$ and reduced time $\tilde{t} = t/T_{max}$.

3. EPSD and spectral moments of the dynamic response

Let us consider a linear elastic SDOF system characterized by mass m, a fundamental circular frequency $\omega_0 = 2\pi n_0$ (being n_0 the natural frequency), damping ratio ξ and displacement x. Its equation of motion is given by:

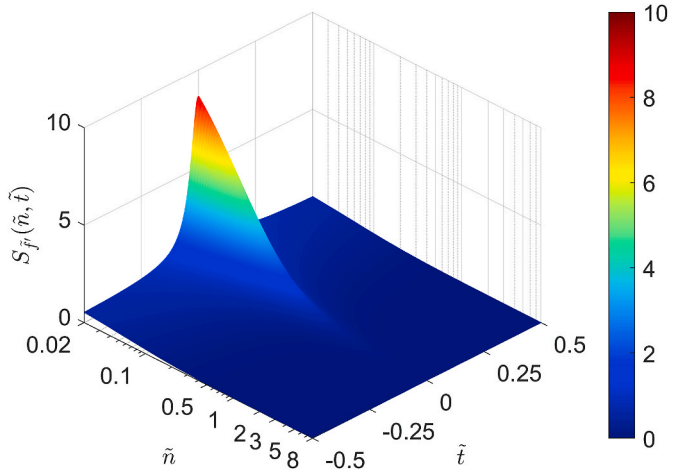

Fig. 1. One-sided EPSD of the reduced fluctuating part of the wind load $\underset{f}{S}$ as a function of the reduced frequency $\tilde{n} = nL_v/\bar{v}_{max}$ and reduced time $\tilde{t} = t/T_{max}$.

$$\ddot{x}(t) + 2\omega_0 \xi \dot{x}(t) + \omega_0^2 x(t) = \frac{1}{m} f(t) \tag{12}$$

where $f(t)$ is defined in Eq. (3) (and characterized by the one-sided EPSD in Eq. (8)). According to the decomposition of the loading in Eq. (4), the dynamic response can be expressed as follows:

$$x(t) = \bar{x}(t) + x'(t) \tag{13}$$

where $\bar{x}(t)$ and $x'(t)$ are the mean and fluctuating part of the response, associated with the mean and fluctuating part of the loading, $\bar{f}(t)$ (Eq. (5)) and $f'(t)$ (Eq. (6)), respectively.

The reduced fluctuating part of the response $\tilde{x}'(t)$ is the solution of Eq. (12), with $f(t)$ substituted by the reduced fluctuating part of the loading (Eq. (7)). It is related to the fluctuating part of the response by the following Equation:

$$\tilde{x}'(t) = \frac{x'(t)}{\left(2C\bar{I}_v \bar{v}^2_{max}\right)} \tag{14}$$

Two possible approaches are outlined for the statistical characterization of the dynamic response, here defined as Rigorous (Section 3.1) and Simplified (Section 3.2) method.

3.1. Rigorous method

The mean part of the response is obtained solving Eq. (12) with $f(t)$ substituted by $\bar{f}(t)$ (Eq. (5)). It is given by:

$$\bar{x}(t) = C\bar{v}^2_{max} \int_{-\frac{T_{max}}{2}}^{t} h(t-\tau)\gamma^2(\tau)d\tau \tag{15}$$

being $h(t)$ the impulse response function of the dynamical system:

$$h(t) = \frac{1}{m\omega_d} e^{-\xi\omega_0 t} \sin(\omega_d t)\mathcal{H}(t) \tag{16}$$

where $\mathcal{H}(t)$ is the Heaviside function and $\omega_d = \omega_0\sqrt{1-\xi^2}$.

The fluctuating part of the response is the solution of Eq. (12) with $f(t)$ substituted by $f'(t)$ (Eq. (6)). Its one-sided EPSD, as outlined in Appendix I, is given by Eq. (54) with $S_{r_0}(n) = \left(2C\bar{I}_v\bar{v}^2_{max}\right)^2 S_{\tilde{v}}(n)$:

$$S_{x'}(n,t) = \left(2C\bar{I}_v\bar{v}^2_{max}\right)^2 |Z(n,t)|^2 S_{\tilde{v}}(n) \tag{17}$$

According to Eqs. (14) and (17) the one-sided EPSD of the reduced fluctuating part of the response reads:

$$S_{\tilde{x}}(n,t) = |Z(n,t)|^2 S_{\tilde{v}}(n) \tag{18}$$

The quantity $Z(n,t)$ in Eqs. (17) and (18) is the EFRF, defined in Appendix I (Eq. (55), with $a(n,t) = \gamma^2(t)$ and changing the integration limits to $\left[-\frac{T_{max}}{2}, t\right]$):

$$Z(n,t) = \int_{-\frac{T_{max}}{2}}^{t} h(t-\tau)e^{i2\pi n\tau}\gamma^2(\tau)d\tau \tag{19}$$

where i is the imaginary unit. As an example, Fig. 2 plots the function $|Z(n,t)|^2$ (Fig. 2a) and the one-sided EPSD of the reduced response $S_{\tilde{x}}(n,t)$ (Fig. 2b) for a SDOF system with $n_0 = 0.2$ Hz and $\xi = 0.2\%$, assuming the wind loading model described in Section 2 (Eq. (10) and (11)).

From Eqs. (17) and (18) it can be deduced that the response is not a uniformly modulated process since the EFRF recouples time and frequency together.

The NGSMs of the reduced fluctuating part of the response are derived following their definitions reported in Appendix I (Eq. (58)) and read:

$$c_{00,\tilde{x}}(t) = \int_0^{+\infty} |Z(n,t)|^2 S_{\tilde{v}}(n)dn \tag{20}$$

$$c_{01,\tilde{x}}(t) = -i\int_0^{+\infty} Z^*(n,t)\dot{Z}(n,t)S_{\tilde{v}}(n)dn \tag{21}$$

$$c_{11,\tilde{x}}(t) = \int_0^{+\infty} |\dot{Z}(n,t)|^2 S_{\tilde{v}}(n)dn \tag{22}$$

Fig. 3 plots, respectively, the spectral moments $c_{00,\tilde{x}}$ (Fig. 3a), $c_{11,\tilde{x}}$ (Fig. 3b) and $c_{01,\tilde{x}'}$ (Fig. 3c and d) evaluated for $n_0 = 0.2$ Hz and $\xi \in [0.2\%, 5\%]$. It can be deduced that, on increasing the damping ratio, the spectral moments $c_{00,\tilde{x}}$, $c_{11,\tilde{x}}$ and the real part of $c_{01,\tilde{x}}$ tend to have a shape similar to the function $\gamma^4(t)$, with a maximum value in the neighbourhood of $t = 0$ s. Moreover, the more the structure is lowly damped, the more the peak of the function is high, while the shape

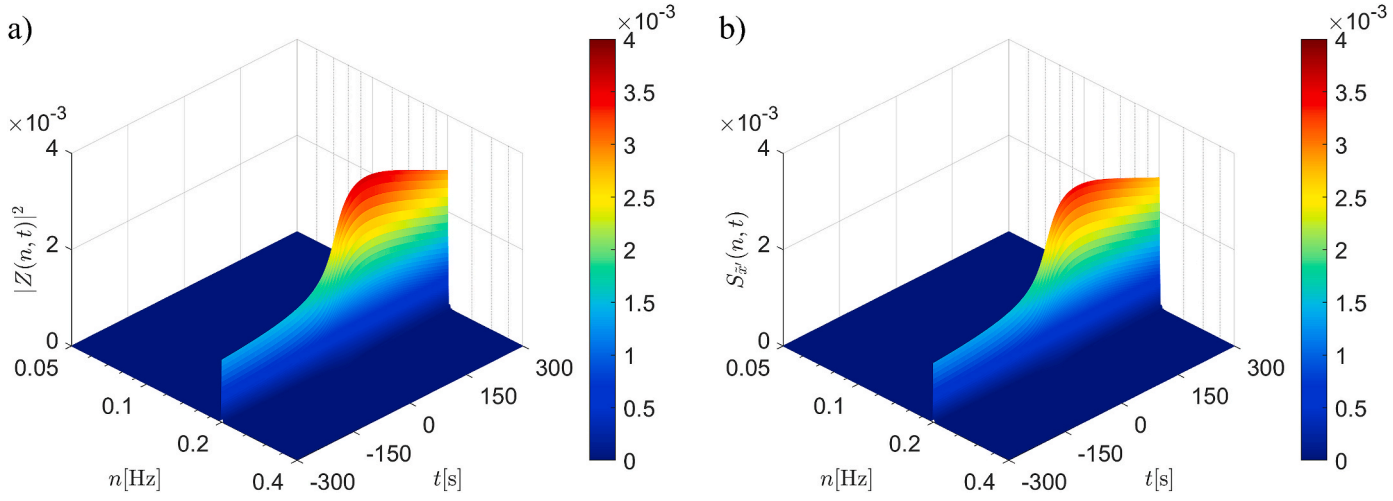

Fig. 2. Rigorous method: Dynamic response of a SDOF system with $n_0 = 0.2$ Hz and $\xi = 0.2\%$: (a) EFRF $|Z(n,t)|^2$; (b) one-sided EPSD of the reduced fluctuating part of the response $S_{\tilde{x}}$.

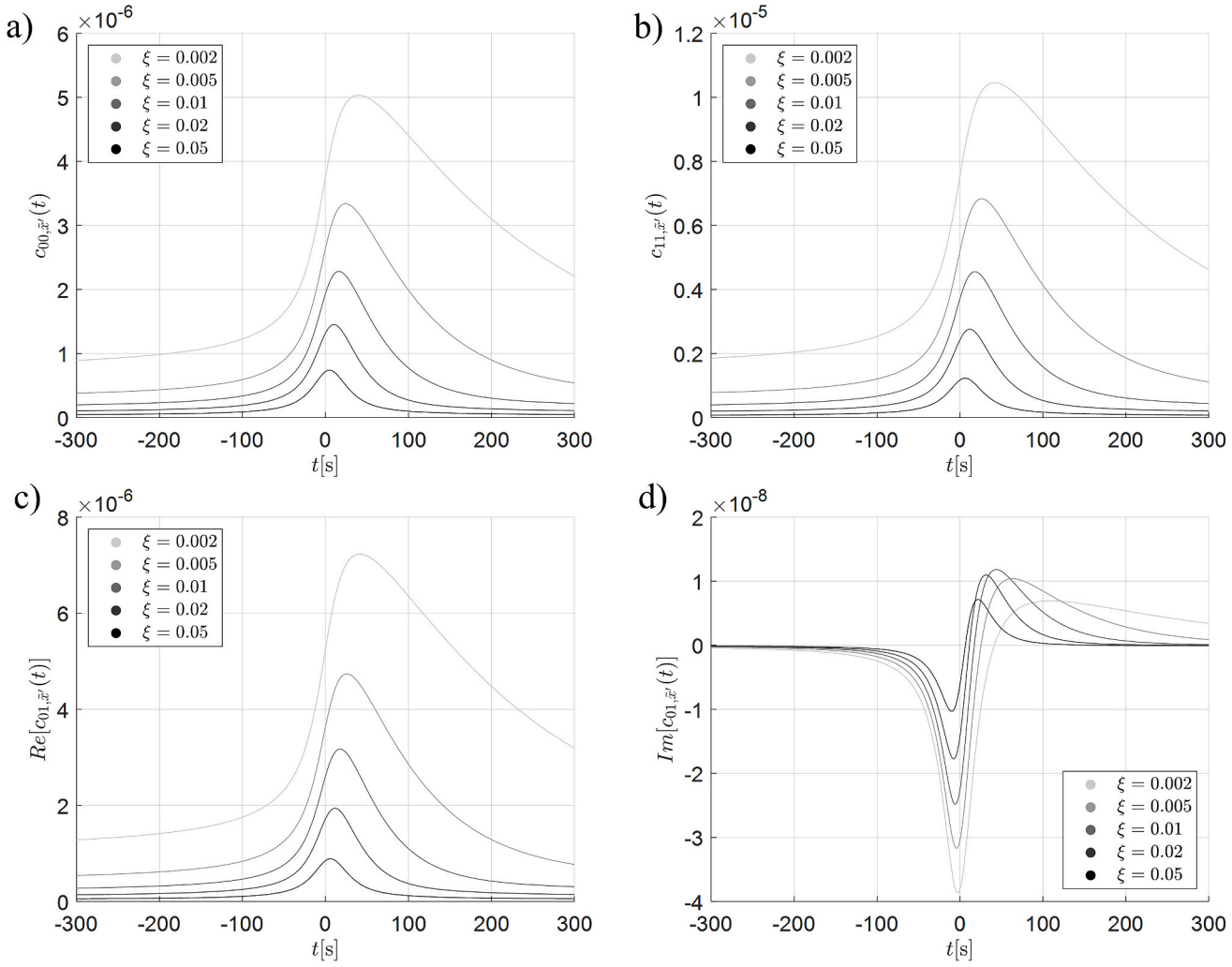

Fig. 3. NGSMs of the dynamic response ($n_0 = 0.2$ Hz): (a) $c_{00,\tilde{x}}$; (b) $c_{11,\tilde{x}}$; (c) Real part of $c_{01,\tilde{x}}$; (d) Imaginary part of $c_{01,\tilde{x}}$.

changes with respect to $\gamma^4(t)$, losing its symmetry with respect to $t = 0$ s. These results are in agreement with the ones observed in literature (Chen, 2008; Huang et al., 2013).

From the NGSMs in Eqs. (20)-(22) the spectral parameters such as the expected frequency, the bandwidth factor and the correlation coefficient, namely $\nu_{\tilde{x}}(t)$, $q_{\tilde{x}}(t)$ and $\rho_{\tilde{x}\tilde{x}}(t)$, are obtained and reported in Appendix I (Eqs. (61)-(63)).

The standard deviation of the reduced fluctuating part of dynamic response is derived from the first NGSM in Eq. (20) as follows:

$$\sigma_{\tilde{x}}(t) = \sqrt{c_{00,\tilde{x}}(t)} \tag{23}$$

According to Eq. (17), the standard deviation of the fluctuating response reads:

$$\sigma_{\tilde{x}'}(t) = 2C\bar{I}_v\bar{v}^2_{max}\sqrt{c_{00,\tilde{x}}(t)} \tag{24}$$

Comparing Eqs. (15) and (24) it is worth to notice that the modulating function of the mean and standard deviation of the response are not the same and hence, in general, their maximum values are not simultaneous. This delicate aspect will be further discussed in the next Sections.

3.2. Simplified method

If T_γ, which is a measure of the duration of the peak of the thunderstorm, is large compared with the memory of the dynamical system, the dynamic effects produced by the modulating function $\gamma(t)$ in the mean and fluctuating parts of the loading can be neglected. This assumption, leading to the Simplified method, can be considered as approximately verified when $T_\gamma > \frac{3}{\xi(2\pi n_0)}$ (Muscolino, 2012), i.e. for stiff and damped systems. Under this hypothesis, the quantity $\gamma^2(t)$ can be moved outside the integrals in Eqs. (15) and (19) and, extending the integration limits to $[-\infty, +\infty]$, $\bar{x}(t)$ and $Z(n,t)$ are given, respectively, by the following expressions (Muscolino and Alderucci, 2015):

$$\bar{x}(t) = \frac{C\bar{v}^2_{max}}{m(2\pi n_0)^2}\gamma^2(t) \tag{25}$$

$$Z(n,t) = \gamma^2(t)e^{i2\pi nt}H(n) \tag{26}$$

where $H(n)$ is the mechanical admittance function:

$$H(n) = \frac{1}{m(2\pi n_0)^2}\frac{1}{1 - \frac{n^2}{n_0^2} + 2i\xi\frac{n}{n_0}} \tag{27}$$

Eq. (25) shows that $\bar{x}(t)$ is the quasi-static response to $\bar{f}(t)$ (Eq. (5)), whilst Eq. (26) shows that, except from a phase angle, the EFRF coincides with the mechanical admittance function $H(n)$ modulated in time by the function $\gamma^2(t)$. The derivation of the one-sided EPSD of the fluctuating response is also straightforward:

$$S_{x'}(n,t) = |H(n)|^2 S_{f'}(n,t) \tag{28}$$

Substituting Eq. (26) into Eq. (18), the one-sided EPSD of the reduced fluctuating part of the response is given by:

$$S_{\underset{\sim}{x}}(n,t) = \gamma^4(t)|H(n)|^2 S_{\underset{\sim}{v}}(n) \tag{29}$$

As an example, Fig. 4 plots the quantity $\gamma^4(t)|H(n)|^2$ and the one-sided EPSD of the reduced fluctuating response $S_{\underset{\sim}{x}}$ for a SDOF system with $n_0 = 0.2$ Hz and $\xi = 0.2\%$.

Eq. (29) shows that, as consequence of the hypothesis of a slowly-varying modulating function, the dynamic response retains the property of being a uniformly modulated process.

The Vanmarcke's spectral moments of the reduced fluctuating response are derived from Eq. (29):

$$\lambda_{0,\underset{\sim}{x}}(t) = \gamma^4(t) \int_0^{+\infty} |H(n)|^2 S_{\underset{\sim}{v}}(n) dn \tag{30}$$

$$\lambda_{1,\underset{\sim}{x}}(t) = \gamma^4(t) \int_0^{+\infty} (2\pi n)|H(n)|^2 S_{\underset{\sim}{v}}(n) dn \tag{31}$$

$$\lambda_{2,\underset{\sim}{x}}(t) = \gamma^4(t) \int_0^{+\infty} (2\pi n)^2|H(n)|^2 S_{\underset{\sim}{v}}(n) dn \tag{32}$$

where $S_{\underset{\sim}{v}}(n)$ is the one sided PSD of the reduced turbulent fluctuations based on frequency n (Eq. (11)). The spectral moments $\lambda_{j,\underset{\sim}{x}}(t)$ ($k = 0, 1, \ldots N$) are thus the ones typical of stationary processes except that they are modulated in time by the function $\gamma^4(t)$. Accordingly, the expected frequency and the bandwidth factor read:

$$\nu_{\underset{\sim}{x}} = \frac{1}{2\pi}\sqrt{\frac{\lambda_{2,\underset{\sim}{x}}(t)}{\lambda_{0,\underset{\sim}{x}}(t)}} \tag{33}$$

$$q_{\underset{\sim}{x}} = \sqrt{1 - \frac{\lambda^2_{1,\underset{\sim}{x}}(t)}{\lambda_{0,\underset{\sim}{x}}(t)\lambda_{2,\underset{\sim}{x}}(t)}} \tag{34}$$

Since the spectral moments $\lambda_{j,\underset{\sim}{x}}(t)$ posses the same modulating function (Eqs. (30)-(32)), the parameters in Eqs. (33) and (34) are not time dependent.

The standard deviation of the reduced fluctuating part of the response is derived from the first spectral moment in Eq. (30) as follows:

$$\sigma_{\underset{\sim}{x}}(t) = \gamma^2(t) J \tag{35}$$

where:

$$J = \sqrt{\int_0^{+\infty} |H(n)|^2 S_{\underset{\sim}{v}}(n) dn} \tag{36}$$

According to Eq. (28), the standard deviation of the fluctuating part of the response reads:

$$\sigma_{x'}(t) = 2C\bar{I}_v \bar{v}^2_{max} \gamma^2(t) J \tag{37}$$

Eqs. (25) and (37) show that both the mean and standard deviation of the dynamic response are modulated in time by the same function, i.e. $\gamma^2(t)$, and hence their maximum values are simultaneous.

4. Expected value of the maximum of the fluctuating response, peak factor and equivalent parameters

The extreme pdf of the nonstationary response can be estimated based on the Poisson or Vanmarcke models taking into account the variation in time of the standard deviation and of the mean part of the response. Then, the mean and standard deviation of the maximum can be derived from its pdf (Hu and Xu, 2014; Huang et al., 2013; Kareem et al., 2019). This procedure is rather unsuitable for rapid engineering calculations due to its lack of handiness. With the objective of extending the gust factor technique to thunderstorm response analysis, an alternative approach is considered based on the definition of suitable parameters able to adapt the gust factor formulation commonly adopted for synoptic winds. In particular, a time interval over which to calculate the peak factor needs to be defined, along with a suitable value of the standard deviation.

This shortcoming can be overcome through the EPT, considering an equivalent stationary process defined through suitable equivalent parameters, with the maximum value that coincides with the one of the original nonstationary process. The EPT was originally developed by Michaelov et al. (2001) for the dynamic response of a linear elastic SDOF system to a nonstationary zero-mean white noise modulated by a deterministic function. The technique is based on the approximation of the cumulative distribution function (CDF) of the extreme value of a nonstationary process by the CDF of a corresponding equivalent stationary process defined through an equivalent standard deviation σ_{eq}

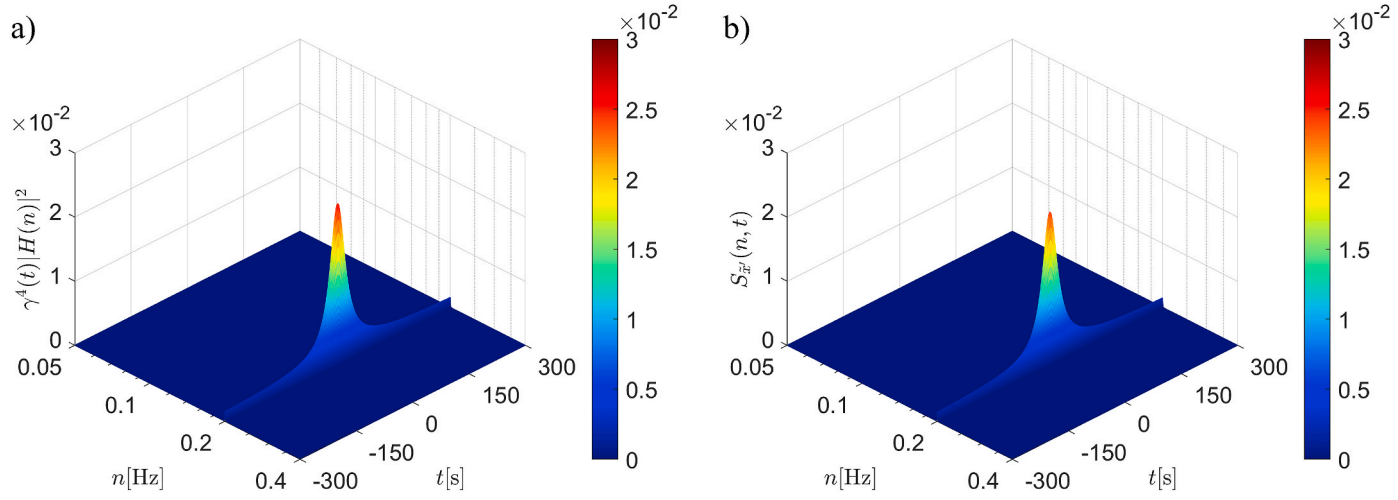

Fig. 4. Simplified method: Dynamic response of a SDOF system with $n_0 = 0.2$ Hz and $\xi = 0.2\%$: (a) Modulated mechanical admittance function; (b) one-sided EPSD of the reduced fluctuating part of the response $S_{\underset{\sim}{x}}$.

and an equivalent period T_{eq}. The EPT was adopted by Kwon and Kareem (2019, 2009) in the framework of the dynamic response of structures subjected to thunderstorm outflows to estimate the maximum of the fluctuating part of the response. According to Michaelov et al. (2001), the maximum value of the reduced fluctuating part of the response is given by:

$$\widetilde{x}'_{max} = g_{\underset{\sim}{x}}\left(\nu_{\underset{\sim}{x}} T_{eq}\right)\sigma_{eq} \tag{38}$$

where $g_{\underset{\sim}{x}}$ is the peak factor and $\nu_{\underset{\sim}{x}}$ is the expected frequency (Eq. (33) and (61)). The peak factor reads (Davenport, 1961):

$$g_{\underset{\sim}{x}}\left(\nu_{\underset{\sim}{x}} T_{eq}\right) = \sqrt{2ln\left(\nu_{\underset{\sim}{x}} T_{eq}\right)} + \frac{0.5772}{\sqrt{2ln\left(\nu_{\underset{\sim}{x}} T_{eq}\right)}} \tag{39}$$

Differently from Michaelov et al. (2001), the peak factor is here evaluated considering $\nu_{\underset{\sim}{x}}$, dropping the factor 2 adopted in the original method. This modification is due to the fact that in this study the dynamic response is not zero-mean, and the maximum values of interest lay on the positive side. As an example, Fig. 5 plots the correlation coefficient $\rho_{\underset{\sim}{x}\,\underset{\sim}{\dot{x}}}$ (Eq. (63)) and the expected frequency $\nu_{\underset{\sim}{x}}$ for a system with $n_0 = 0.2$ Hz and $\xi \in [0.2\%,\ 5\%]$.

Fig. 5a shows that the correlation coefficient $\rho_{\underset{\sim}{x}\,\underset{\sim}{\dot{x}}}$ is very small. This result, valid also for other fundamental frequencies between 0.05 and 3 Hz, allows to neglect the correlation between $\widetilde{x}'$ and $\dot{\widetilde{x}}'$ (Michaelov et al., 2001) with a certain margin of conservatism as outlined by Kwon and Kareem (2013). Concerning the normalized expected frequency (Fig. 5b), its trend is almost constant except a small variation in a neighbourhood of $t = 0$ s due to the misalignment of the peaks of $c_{00,\underset{\sim}{x}}(t)$ and $c_{11,\underset{\sim}{x}}(t)$.

The equivalent parameters in Eq. (38) are given by (Michaelov et al., 2001):

$$\sigma^2_{eq}(\eta) = \frac{\int_{-\frac{T_{max}}{2}}^{+\frac{T_{max}}{2}} \left[\sigma^2_{\underset{\sim}{x}}(t)\right]^{\eta+1} dt}{\int_{-\frac{T_{max}}{2}}^{+\frac{T_{max}}{2}} \left[\sigma^2_{\underset{\sim}{x}}(t)\right]^{\eta} dt} \tag{40}$$

$$T_{eq}(\eta) = \exp\left(\eta\right) \int_{-\frac{T_{max}}{2}}^{+\frac{T_{max}}{2}} \exp\left(-\frac{\eta\sigma^2_{eq}}{\sigma^2_{\underset{\sim}{x}}(t)}\right) dt \tag{41}$$

$$q_{eq} = \frac{\sigma_{eq}}{T_{eq}} \exp\left(\frac{\widehat{x}^2}{2\sigma^2_{eq}}\right) \int_{-\frac{T_{max}}{2}}^{+\frac{T_{max}}{2}} \frac{q_{\underset{\sim}{x}}(t)}{\sigma_{\underset{\sim}{x}}(t)} \exp\left(-\frac{\widehat{x}^2}{2\sigma^2_{\underset{\sim}{x}}(t)}\right) dt \tag{42}$$

In Eqs (40) and (41) η is a parameter fixed a-priori (Michaelov et al., 2001): in this study the value $\eta = 4$ is adopted. The parameter q_{eq} in Eq. (42) is the equivalent bandwidth factor and it is derived in Michaelov et al. (2001) by introducing the Vanmarcke approximation. The bandwidth factor $q_{\underset{\sim}{x}}$ is evaluated by means of Eq. (62) while the recommended value for the parameter $\widehat{x}$ is $\widehat{x} = g_{\underset{\sim}{x}}\sigma_{eq}$ (Michaelov et al., 2001). For the purposes of the study, $\widehat{x}$ has been calculated adopting the expected frequency $\nu_{\underset{\sim}{x}}$ calculated at the time instant when $c_{00,\underset{\sim}{x}}(t)$ is maximum. This choice is justified by the fact that, as shown in Fig. 5b, the expected frequency does not show significant variations in time and the maximum value of $c_{00,\underset{\sim}{x}}(t)$ occurs in the middle of the small variation of $\nu_{\underset{\sim}{x}}$.

Coherently with the approach normally adopted in wind engineering, Eq. (38) implicitly identifies the maximum response with its expected value. This assumption was shown to be questionable dealing not only with the dynamic response to thunderstorm winds (Solari et al., 2017) but also for the dynamic response to synoptic winds (Piccardo et al., 2018) since, in both cases, the extreme pdf results rather spread when the damping ratio becomes significantly small. However, with the aim of following the traditional approach focusing on the mean value of the maximum, this hypothesis has been assumed in the study. Research is currently ongoing to investigate whether the mean value may be considered representative of the maximum or if this assumption is not reliable in some cases.

The following Sections outline the calculation of the equivalent parameters following both the Rigorous and Simplified method for a set of

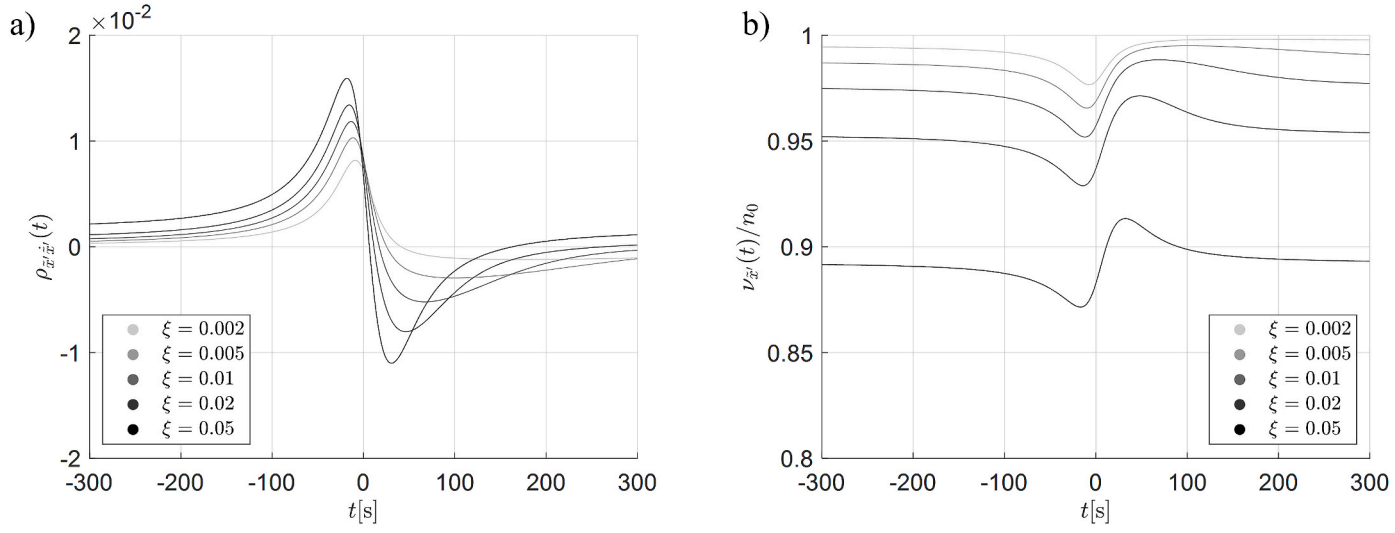

Fig. 5. Rigorous method ($n_0 = 0.2$ Hz): (a) correlation coefficient between x' and $\dot{x}'$; (b) normalized expected frequency.

SDOF systems. It is worth to point out that the EPT here employed is an approximated procedure to estimate the maximum. The statement "Rigorous" method is therefore used to identify the approach discussed in Section 3.1 for which the EPSD of the response and the NGSMs are derived following a rigorous procedure, accounting for the transient dynamic effects through the EFRF.

4.1. Rigorous method

According to Eqs. (23) and (40)-(42), the evaluation of the equivalent parameters requires the estimate of the NGSMs in Eqs. (20)-(22) which are employed for the calculation of the equivalent standard deviation σ_{eq}, substituting Eq. (23) into Eq. (40). Successively, the equivalent time interval T_{eq} is derived replacing σ_{eq} and Eq. (23) into Eq. (41). Finally, the two parameters are adopted to calculate the equivalent bandwidth factor q_{eq} according to Eq. (42).

Fig. 6 plots the equivalent parameters σ_{eq} and T_{eq} (Eq. (40) and (41)) for $n_0 \in [0.05,\ 3]$ Hz and $\xi \in [0.2\%,\ 5\%]$.

It can be observed that both the parameters show decreasing trends on increasing the fundamental frequency of the system and the damping ratio. The trend of σ_{eq} remains very similar for all the damping ratios considered and its behaviour is in accordance with the standard deviation of the response which reduces on increasing the natural frequency and the damping ratio.

The trend of T_{eq} shows remarkable differences varying the damping ratio. On increasing it, the curves shift to the left. Furthermore, an upper and lower bound are detectable: the former is reached for very low frequencies and damping ratios and lays in a neighbourhood of $T_{eq} = 300$ s, which is half of the total time interval $T_{max} = 600$ s, while the latter corresponds to high natural frequencies and lays in a neighbourhood of $T_{eq} = 41.34$ s. The parameter T_{eq} represents the time interval in which the equivalent stationary process is defined and hence within which the maximum of the process of interest is searched. Hence for a flexible and lowly-damped structure, since the width of the temporal region of the peak of the standard deviation is wider, it is reasonable to expect the maximum of the response in a larger time interval and thus the duration of the equivalent stationary process is longer; on the other hand, for a stiff and damped structure, its response is closer to the static one and the maximum is expected in a shorter time interval which does not depend on the mechanical properties of the system.

Moreover, it is clear that the values of T_{eq} are much lower than the traditional 600 s considered for extra-tropical cyclones. For this reason, the pdf of the maximum response is expected to be more spread as pointed out by Solari et al. (2017) and hence the identification of the maximum with its mean value may be less accurate.

Fig. 7 plots the time varying bandwidth factor $q_{\breve{x}}(t)$ calculated for $n_0 = 0.2$ Hz and $\xi \in [0.2\%,\ 5\%]$ (Fig. 7a) and the equivalent bandwidth factor q_{eq} (Eq. (42)), evaluated for $n_0 \in [0.05,\ 3]$ Hz and $\xi \in [0.2\%,\ 5\%]$ (Fig. 7b).

In Fig. 7a $q_{\breve{x}}(t)$ reports steady trends except small variations around $t = 0$ s that increase on decreasing damping ratio, whilst the equivalent bandwidth factor (Fig. 7b) shows a regular behaviour, increasing on increasing the natural frequency and the damping ratio of the system. Overall, Fig. 7 shows that the equivalent bandwidth factor reports very low values for small damping ratios. Indeed, for $\xi = 0.2\%$ the equivalent bandwidth factor remains lower than 0.2, suggesting that the response is significantly narrowband. These results, in accordance with the ones observed for $q_{\breve{x}}(t)$, suggest that the Poisson approximation may lead to conservative results in the evaluation of the maximum of the response for lowly-damped systems.

4.2. Simplified method

The derivation of the equivalent parameters with the Simplified method does not require the calculation of the NGSMs but merely involves the Vanmarcke's spectral moments in Eqs (30)-(32) that are all modulated in time by $\gamma^4(t)$, hence the time-varying nature of these spectral moments does not depend on the mechanical properties of the structure. For this reason, the parameter T_{eq} is unique for any n_0 and ξ considered and, substituting Eq. (30) in Eqs. (40) and (41), after very simple algebra, it follows:

$$\sigma_{eq}^2(\eta) = J^2 \sigma_{eq,\gamma}^2(\eta) \tag{43}$$

$$T_{eq}(\eta) = \exp\left(\eta\right) \int_{-\frac{T_{max}}{2}}^{+\frac{T_{max}}{2}} \exp\left(-\frac{\eta \sigma_{eq,\gamma}^2}{\gamma^4(t)}\right) dt \tag{44}$$

where $\sigma_{eq,\gamma}^2$ is defined as:

$$\sigma_{eq,\gamma}^2(\eta) = \frac{\int_{-\frac{T_{max}}{2}}^{+\frac{T_{max}}{2}} [\gamma^4(t)]^{\eta+1} dt}{\int_{-\frac{T_{max}}{2}}^{+\frac{T_{max}}{2}} [\gamma^4(t)]^{\eta} dt} \tag{45}$$

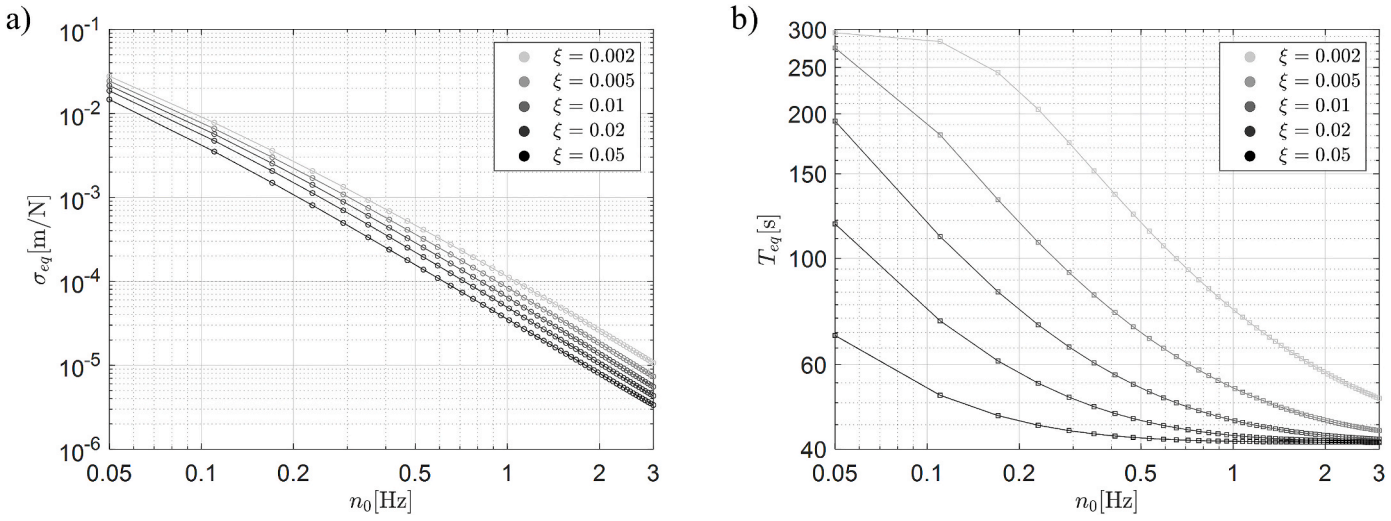

Fig. 6. Rigorous method: equivalent parameters for the estimate of the expected value of the maximum of the response: (a) equivalent standard deviation; (b) equivalent time interval.

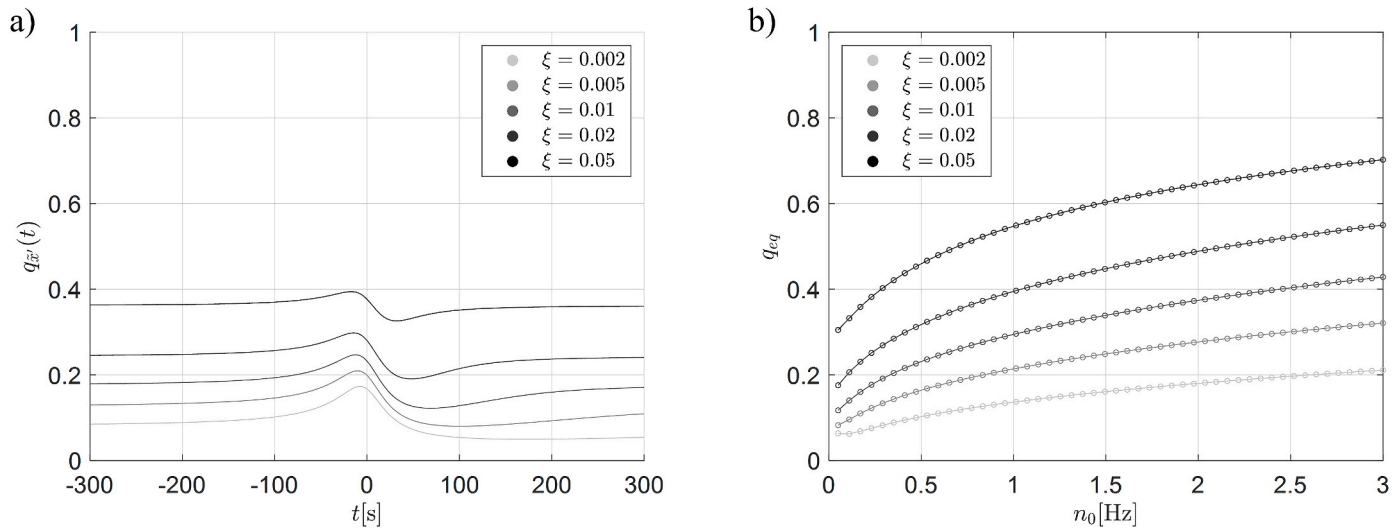

Fig. 7. Bandwidth factor: (a) time varying bandwidth factor calculated for $n_0 = 0.2$ Hz; (b) **e**quivalent bandwidth factor evaluated for the whole set of SDOF systems.

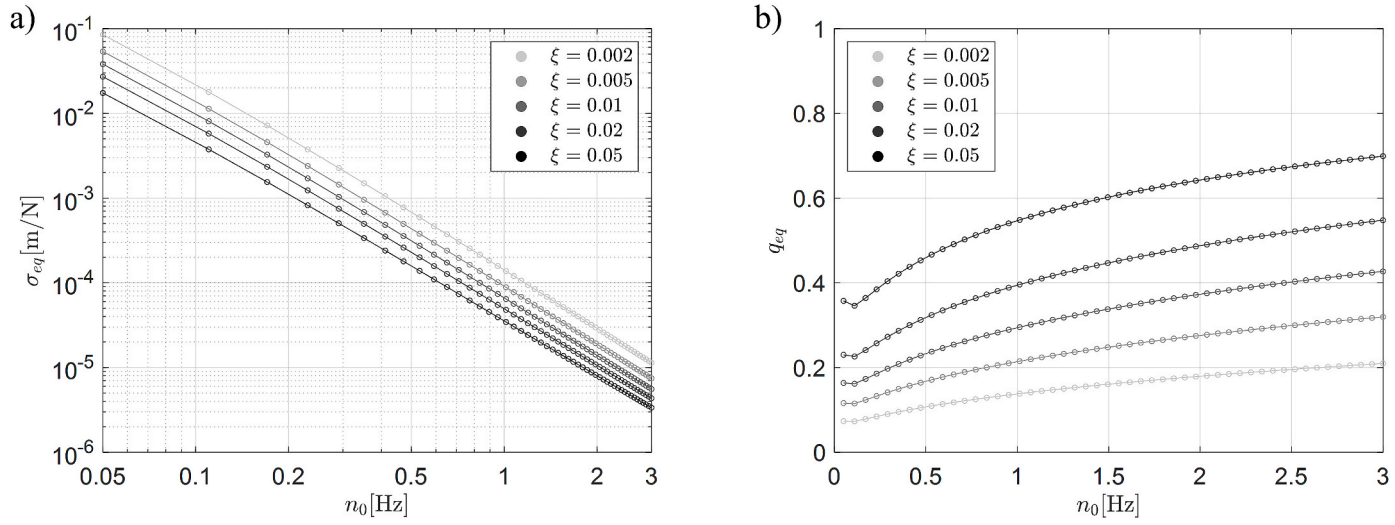

Fig. 8. Equivalent parameters for the Simplified method evaluated for the whole set of SDOF: (a) equivalent standard deviation; (b) equivalent bandwidth factor.

which is independent on the mechanical properties of the system.

Substituting Eq. (10) into Eqs. (44) and (45) and setting $\eta = 4$, the equivalent time interval results $T_{eq} = 41.34$ s. This value coincides with the lower bound estimated through the Rigorous method (Fig. 6).

Fig. 8 reports the trends of the parameters σ_{eq} and q_{eq} for $n_0 \in [0.05, 3]$ Hz and $\xi \in [0.2\%, 5\%]$.

The trends of σ_{eq} in Fig. 8a are very similar to the ones obtained with the Rigorous method (Fig. 6) except that at very low frequencies the Simplified method leads to greater values. In said region only for large damping ratios the two methods give similar values. Concerning the parameter q_{eq} (Fig. 8b), the curves obtained are almost the same of the ones of the Rigorous method, again with the exception for very low frequencies in which Fig. 8b reports slightly higher values.

5. Revised Der Kiureghian method for thunderstorms outflows

In Section 4 it has been shown that, for low values of damping ratio, the fluctuating part of the response is a narrowband random process. Hence, the direct application of the Davenport's formulation of the peak factor may lead to excessive overestimation of the mean value of the maximum fluctuating response.

To overcome this shortcoming, Michaelov et al. (2001) suggest the use of a so-called effective zero-crossing rate (or equivalent expected frequency) ν_e introduced by Der Kiureghian (1980) for which empirical equations were provided. However, Der Kiureghian formulation applies to the dynamic response of SDOF systems excited by stationary white noise inputs, rather different from the case under study in which the excitation is not a white noise. For this reason, an effective zero-crossing rate suitable for the dynamic response to thunderstorm outflows is here derived following the same procedure adopted by Der Kiureghian (1980), using a total of 129 real-scale thunderstorm records (Roncallo and Solari, 2020) as loading condition for the set of SDOF systems considered. From each wind velocity record available, the reduced turbulent fluctuation is extracted and the normalized nonstationary fluctuation of the wind load is obtained from Eq. (7). The dynamic response is therefore evaluated in time domain for the whole set of SDOF systems (with $n_0 \in [0.05, 3]$ Hz and $\xi \in [0.2\%, 5\%]$) by solving the equation of motion in state space. Hence the maximum response is extracted from each time history and the mean value $\mu_{\breve{x},max}$ evaluated per each SDOF system among the maxima of the dynamic responses to each thunderstorm.

Through the parameters derived in the previous Section, the

numerically estimated peak factor $g_{\underset{\sim}{x},num} = \mu_{\underset{\sim}{x},max}/\sigma_{eq}$ is calculated and plotted versus the product $\nu_{\underset{\sim}{x}} T_{eq}$, similarly to Der Kiureghian (1980). Successively, the effective zero-crossing rate ν_e is evaluated fitting the Davenport formulation for the peak factor with the values of $g_{\underset{\sim}{x},num}$, deriving a dimensionless parameter ε such that:

$$\nu_e = \varepsilon \nu_{\underset{\sim}{x}} \tag{46}$$

$$g_{\underset{\sim}{x},num} = \sqrt{2ln(\nu_e T_{eq})} + \frac{0.5772}{\sqrt{2ln(\nu_e T_{eq})}} \tag{47}$$

The parameter ε scales the expected frequency $\nu_{\underset{\sim}{x}}$ to obtain the effective zero-crossing rate ν_e (Eq. (46)), which allows to apply the Davenport peak factor (Eq. (39)) removing the overestimations due to the Poisson assumption. The analyses are carried out separately in Sections 5.1 and 5.2 for the Rigorous and Simplified method, respectively.

5.1. Rigorous method

As discussed in Section 4.1, following the Rigorous method the parameter T_{eq} varies with n_0 and ξ, hence the variation of the product $\nu_{\underset{\sim}{x}} T_{eq}$ depends on the mechanical properties of the system through both parameters. With this premise, Fig. 9 plots the numerically estimated peak factor as a function of the product $\nu_{\underset{\sim}{x}} T_{eq}$, for fixed values of the damping ratio, along with the one provided by Davenport formulation (dashed line).

From Fig. 9 it can be deduced that for all the damping ratios considered, the Davenport formulation provides a reliable approximation of the peak factor for small values of $\nu_{\underset{\sim}{x}} T_{eq}$. For very small damping ratios the numerically estimated peak factor tends to become less dependent on $\nu_{\underset{\sim}{x}} T_{eq}$, assuming very small values. It is worth noting that in these cases the process tends to become narrowband and thus the Poisson assumption is no longer reliable, leading to conservative results when the Davenport formulation is used. On the other hand, for $\xi = 2-5$ % the numerically estimated peak factor is close to the one provided by Davenport formulation.

Following the approach developed in Der Kiureghian (1980), the curves in Fig. 9 have been fitted according to Eq. (47) to derive the parameter ε. Fig. 10 plots the parameter ε derived from the fitting procedure as a function of $\nu_{\underset{\sim}{x}} T_{eq}$, along with its average trends (dashed lines), for fixed values of the damping ratio.

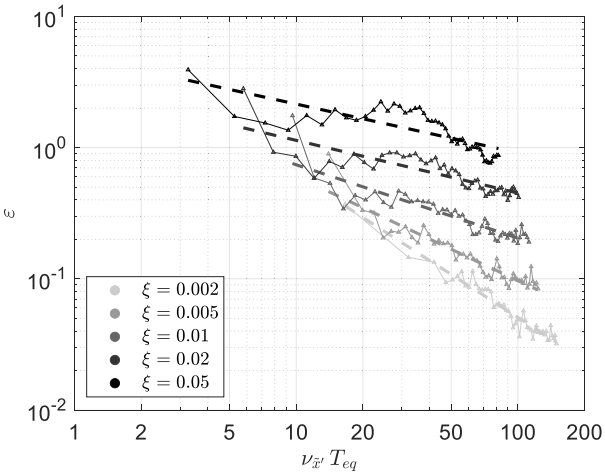

Fig. 10. Trends for the parameter ε derived from data (dots) and its average trends (dashed lines).

In Fig. 10 the average trends show a good fit especially for low ξ and high $\nu_{\underset{\sim}{x}} T_{eq}$, where the correction is of major interest. On the other hand, for higher damping ratios and lower $\nu_{\underset{\sim}{x}} T_{eq}$ the fit is less accurate. However, in these cases the correction is less important since the original Davenport expression for the peak factor leads to acceptable results.

5.2. Simplified method

Differently from the Rigorous case, in the Simplified method the parameter T_{eq} is independent on the dynamic properties of the SDOF system, hence the variation of the product $\nu_{\underset{\sim}{x}} T_{eq}$ is related to the variation of the expected frequency $\nu_{\underset{\sim}{x}}$, which is independent on the modulating function (Eq. (33)). Fig. 11 plots the numerically estimated peak factor as a function of $\nu_{\underset{\sim}{x}} T_{eq}$ for the Simplified method, compared with the Davenport formulation (dashed line).

The curves depicted in Fig. 11 are different from the ones reported for the Rigorous method (Fig. 9), with the major differences for low values of the quantity $\nu_{\underset{\sim}{x}} T_{eq}$ and hence for low $\nu_{\underset{\sim}{x}}$. Firstly, the trends reported are slightly stretched towards lower values of $\nu_{\underset{\sim}{x}} T_{eq}$ if

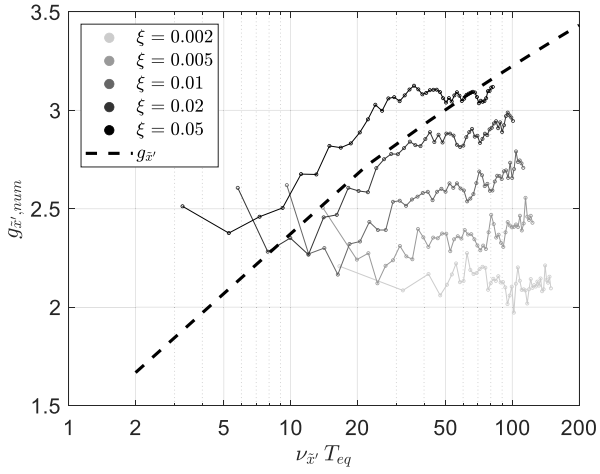

Fig. 9. Rigorous method: $g_{\underset{\sim}{x},num}$ evaluated for the whole set of SDOF considered, compared with the Davenport formulation (dashed line).

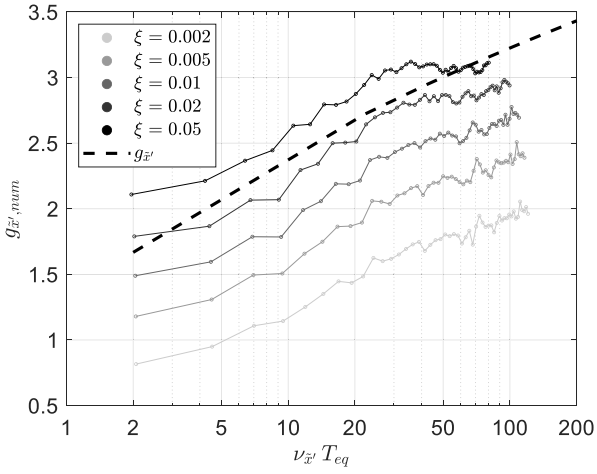

Fig. 11. Simplified method: $g_{\underset{\sim}{x},num}$ evaluated for the whole set of SDOF considered, compared with the Davenport formulation (dashed line).

compared with Fig. 9. Moreover, while for higher $\underset{\sim}{\nu}_x T_{eq}$ the trend is similar to the ones from the Rigorous method, for lower $\underset{\sim}{\nu}_x T_{eq}$ their behaviour is significantly different. Said differences are due to the fact that the Simplified method furnishes higher values of σ_{eq} for flexible and lowly-damped systems, consequently reducing the ratio $\underset{\sim}{\mu}_{x,max} / \sigma_{eq}$. The detachment of the curves from the Davenport formulation in Fig. 11 stresses the reason of the failing of the Simplified method when applied for flexible and lowly-damped systems where the hypothesis of slowly-varying $\gamma^2(t)$ is no longer reliable, leading to excessive overestimations.

The lines in Fig. 11 were fitted according to Eq. (47) in order to derive the dimensionless parameter ε. In this regard, it is worth to notice that, differently from Fig. 9, the lines in Fig. 11 have the same trend, nearly shifted depending on the damping ratio. Moreover, they possess a trend very similar to the one from the Davenport formulation. For these reasons, it is reasonable to search for a unique value of the parameter ε per each damping ratio considered (it should be observed that the importance of the correction is in this case limited to the higher fundamental frequencies and hence to higher $\underset{\sim}{\nu}_x T_{eq}$, since the application of the Simplified method itself is not valid for more flexible systems).

The fit has been performed within the limits of applicability of the Davenport's formulation for the peak factor, i.e. $\underset{\sim}{\nu}_x T_{eq} > 1$, considering only the values $\underset{\sim}{g}_{x,num} \geq 1.67$. Fig. 12 plots the ε parameter evaluated per each damping ratio.

Fig. 12 shows a linear trend of the parameter ε with values higher than the unity for $\xi = 5$ %, coherent with the curves in Fig. 11. It should be pointed out that in this case the parameter ε is identified with its raw values instead of a fitting procedure as the case of the Rigorous method. Hence the correction through the effective zero-crossing rate ν_e in the Simplified method is apported in a more targeted manner.

6. Maximum value of the dynamic response and numerical validation with real thunderstorm records

In this section, after a discussion about the contemporaneity of the maxima of the mean and fluctuating parts (Section 6.1), the maximum value of the dynamic response is calculated analytically as the sum of these two contributions. The maximum dynamic response estimated according to the developed procedure is validated against the mean value of the maximum response numerically calculated in time domain, employing as loading condition the thunderstorm records available, discussing the performance of the Rigorous and Simplified method. The comparison is reported in terms of mean reduced response spectrum

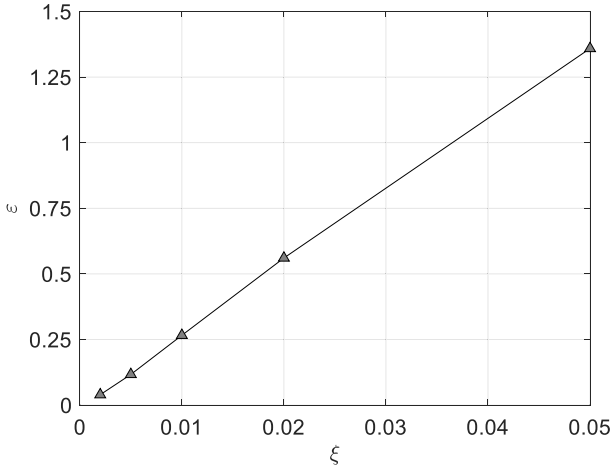

Fig. 12. Dimensionless parameter ε.

(Solari et al., 2015b) including the correction proposed with the effective zero-crossing rate.

6.1. Maximum value of the dynamic response

The maximum value of the dynamic response should be derived by recombining the maxima of its mean and fluctuating parts which do not necessarily occur simultaneously. In order to establish a proper rule for the recombination of the maxima some aspects are worth to be discussed. Firstly, when the system is stiff and sufficiently damped, the dynamic response is quasi-static and hence the modulating functions of the mean and standard deviation of the response coincide. In this case, the maximum of the fluctuating part of the response is reasonably expected in a neighbourhood of the peak of the modulating function and the two can be considered simultaneous. However, this hypothesis does not hold for the more general case since the modulating functions of the mean and fluctuating part of the dynamic response are different, as pointed out in Section 4, and estimating the maximum response adding up the maxima of the mean and fluctuating response could lead to conservative results. As an example, Fig. 13 plots the time histories of the dynamic response of two different linear SDOF systems to two examples of thunderstorm events. Fig. 13 c,d refer to a flexible lowly-damped SDOF system ($n_0 = 0.05$ Hz, $\xi = 0.2$%), Fig. 13 e,f refer to a stiffer and more damped system ($n_0 = 3$ Hz, $\xi = 5$ %). In Fig. 13 c,d,e,f the quantities x_{max}, $\overline{x}_{max}$, x'_{max} are the maxima of the dynamic response, of the mean and fluctuating part, respectively.

It can be observed that, for the flexible and lowly-damped system, the maximum of the fluctuating part of the response is not simultaneous with the maximum of the mean part (Fig. 13c and d). In this framework, while in the first event the maximum response occurs close to the maximum of its mean part (Fig. 13c), in the second event also the maximum response occurs later and coincides with the maximum of the fluctuating part. On the other hand, for both events, the maximum of the mean and fluctuating part of the response of the stiff system occur simultaneously, along with the maximum response (Fig. 13e and f). Moreover, it can be observed that the maximum of the mean part occurs in a neighbourhood of the peak of the loading in all the cases considered. Thus, the dynamic effects concerning the mean part of the response are negligible, and the maximum value of the mean part of the response can be evaluated as the maximum of Eq. (25).

In order to recombine the maxima of the mean and fluctuating part of the response the possibility of direct summation of the two quantities is investigated. This approach implicitly assumes that the two maxima are simultaneous and can be overconservative. The amount of the error committed is estimated calculating in time domain the quantities x_{max}, $\overline{x}_{max}$, x'_{max} for a set of SDOF systems subjected to the wind load (Eq. (3), (5) and (6)) provided by the thunderstorm data available (Roncallo and Solari, 2020). Fig. 14 plots the average of the ratios between the recombination of the maxima ($\overline{x}_{max} + x'_{max}$) and x_{max} per each system considered.

Fig. 14 shows that the overestimation provided decreases on increasing n_0 and ξ and remains confined between 5% and 10% for all the damping ratios considered, except for very flexible structures for which the error rises to 35% for lowly damped systems. It should be noticed that very low values of natural frequencies can characterize particularly flexible structures, such as long span bridges for which specific analyses may be addressed, but overall the approach gives a good estimation. In view of this result, the two maxima can be recombined as follows:

$$x_{max} = \overline{x}_{max} + 2C\overline{I}_v \overline{v}^2_{max} \underset{\sim}{g}_x \left(\underset{\sim}{\nu}_x T_{eq}\right) \sigma_{eq} \tag{48}$$

6.2. Validation against real recorded thunderstorms

The validation of the approach developed is carried out against the mean value of the maximum response numerically calculated in time

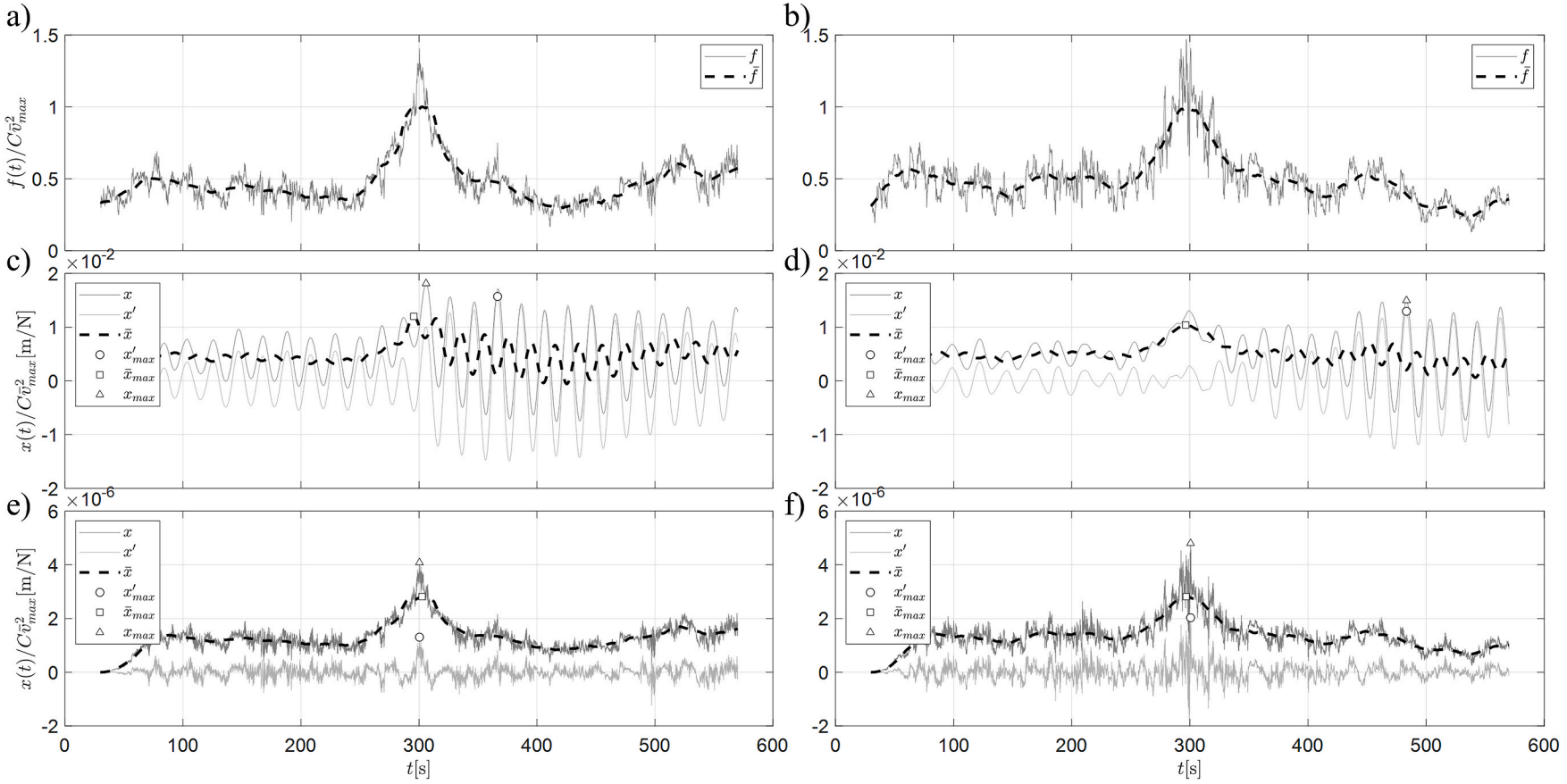

Fig. 13. Dynamic response to two recorded thunderstorm events: (a), (b) normalized wind load; (c), (d) dynamic response of a flexible and lowly damped SDOF system ($n_0 = 0.05$ Hz, $\xi = 0.2$ %); (e), (f) dynamic response of a stiff and damped SDOF system ($n_0 = 3$ Hz, $\xi = 5$ %).

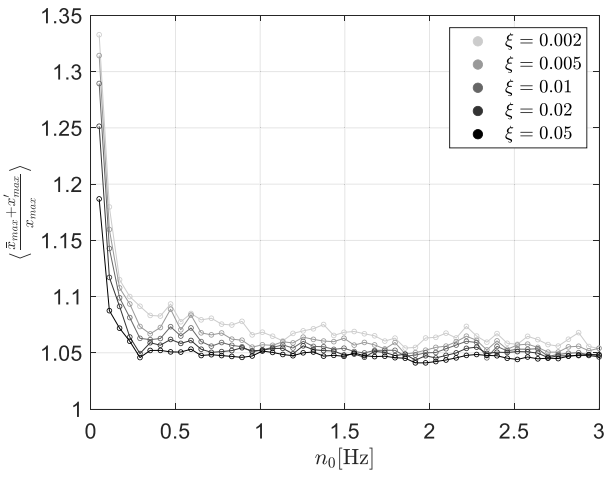

Fig. 14. Error in the recombination of the maximum dynamic response.

domain, employing as loading condition the thunderstorm records available. In particular, for each fundamental frequency and damping ratio considered the dynamic response to the 129 thunderstorm records is calculated and the mean of the maxima derived. Since this quantity, suitably normalized, coincides with the response spectrum (RS) from Solari et al. (2015b) and Solari (2016), the comparison is shown in a more suitable form normalizing the maximum of the response with the maximum of its mean part. This ratio is defined as mean reduced RS and reads (Solari et al., 2015b):

$$S_{\overline{d}} = \frac{x_{max}}{\overline{X}_{max}} \tag{49}$$

where $\overline{X}_{max}$ is the static response to the loading due to the maximum value of the mean wind velocity:

$$\overline{X}_{max} = \frac{C\overline{v}_{max}^2}{m(2\pi n_0)^2} \tag{50}$$

The mean reduced RS is derived according to the definitions of the maximum response in Eq. (48). It is worth noticing that the mean reduced RS takes the role of the gust factor of the response.

Substituting Eqs. (48) and (50) into Eq. (49), the mean reduced RS is written in the following form:

$$S_{\overline{d}} = 1 + 2m(2\pi n_0)^2 \overline{I}_v g_{\underset{\sim}{x}}\left(\nu_{\underset{\sim}{x}}, T_{eq}\right)\sigma_{eq} \tag{51}$$

The mean value of the mean reduced RS is defined as follows:

$$\langle S_{\overline{d}} \rangle = 1 + 2m(2\pi n_0)^2 \langle \overline{I}_v \rangle g_{\underset{\sim}{x}}\left(\nu_{\underset{\sim}{x}}, T_{eq}\right)\sigma_{eq} \tag{52}$$

where $\langle \overline{I}_v \rangle$ is the mean value of $\overline{I}_v$.

To apply the correction introduced in Section 5 is sufficient to substitute in Eq. (52) the expected frequency with the effective zero-crossing rate (Eq. (46)). Accordingly, the mean reduced RS is calculated following both the Rigorous and Simplified method substituting the equivalent parameters and the mean value of the turbulence intensity, namely $\langle \overline{I}_v \rangle = 0.12$, in Eq. (52). Fig. 15 compares the numerically estimated mean reduced RS (from the thunderstorm data available (Roncallo and Solari, 2020), circles) with the ones obtained through Eq. (52) applying both the Rigorous (solid lines) and the Simplified method (dashed lines). In particular, Fig. 15a plots the comparison without introducing any correction to the zero-crossing rate, while Fig. 15b plots the comparison relying on the effective zero-crossing rate defined in Section 5.

Fig. 15a shows that the Simplified method overestimates the mean reduced RS with respect to the Rigorous method, especially for flexible systems and low damping ratios. Nevertheless, it can be observed that the more the system is stiff and damped the more the Rigorous and Simplified methods provide comparable results. In particular, it can be deduced that the dynamic response provided by the two methods is the same when $\xi n_0 > \frac{1}{2T_\gamma}$. In this regard, it can be deduced that the results provided by the two methods coincide at every fundamental frequency for $\xi = 5$ %. This result stresses the fact that the Simplified method is in general conservative for the calculation of the maximum dynamic response. Nevertheless, both the EPSD-based RS, compared with the numerically estimated RS, furnish significant overestimations even for stiff systems, except for large values of the damping ratio.

Fig. 15b shows that the introduction of the effective zero-crossing rate significantly improves the agreement between the numerically estimated mean reduced RS and the one derived from the EPSD model. Focusing on the Rigorous method, some residual overestimations are detectable, especially for low damping ratios and low natural frequencies. These overestimations can be due to the hypothesis of constant turbulence intensity, embedded in the modelling of the wind velocity as pointed out in Section 2, and are enhanced by the addition between the maximum values of the mean and fluctuating part of the response since, as outlined in Section 6.1, they may not be simultaneous. Concerning the

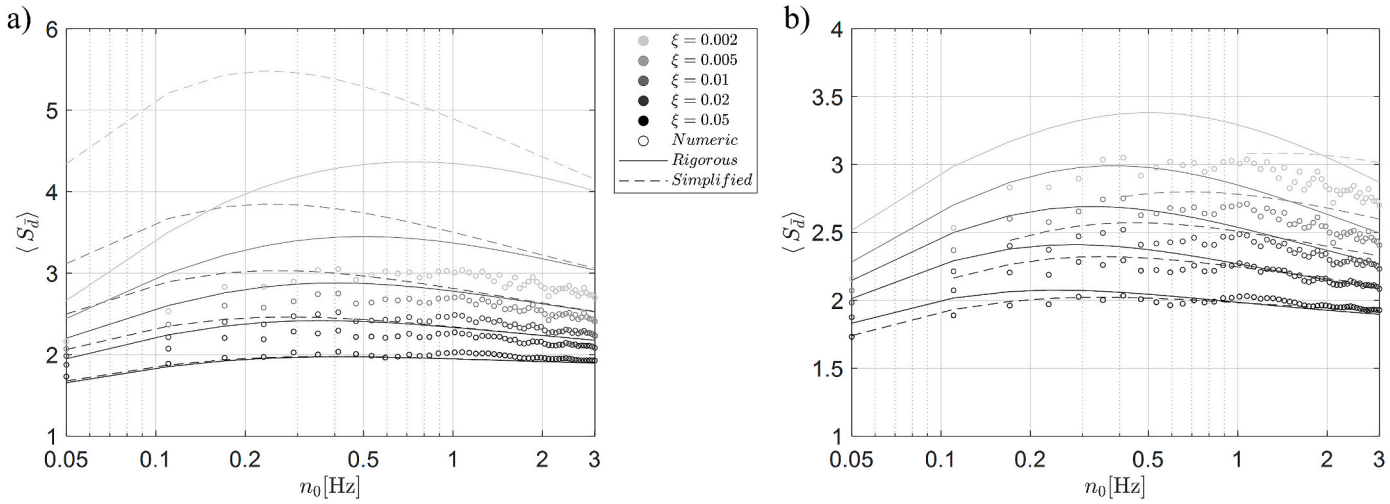

Fig. 15. Mean reduced RS: comparison between numerical results (circles), Rigorous method (solid lines) and Simplified method (dashed lines): (a) Eq. (52), (b) Eq. (52) with effective zero-crossing rate.

Simplified method, the agreement with numerical results is satisfactory although its application is limited to a certain region of fundamental frequencies depending on the damping ratios except for the case of $\xi = 5$ %. It is worth to notice that the Simplified method, where applicable, generally offers a better agreement with numerical results if compared with the Rigorous one for low natural frequencies. This circumstance is due to a compensation between the underestimation of the peak factor for flexible systems associated with introduction of the effective zero-crossing rate and the overestimation of the standard deviation given by the hypothesis of constant turbulence intensity. At higher fundamental frequencies, where the correction through the effective zero-crossing rate is more accurate, the Simplified Method is less reliable than the Rigorous one providing a significant overestimation of the numerically-estimated RS.

7. Conclusions

The present paper studied the reliability of a procedure based on a consistent evolutionary model of the wind velocity for the estimate of the mean value of the maximum response of a wide set of SDOF systems subjected to thunderstorms outflows.

Thunderstorm wind velocity has been schematized as the superimposition of a deterministic slowly-varying mean and a fluctuating component, modelled as a uniformly modulated nonstationary random process. The dynamic response is also decomposed as the superimposition of the deterministic response to the slowly-varying mean and a random nonstationary component, that is not uniformly modulated. A simplified formulation is also applied, based on the assumption of slowly-varying modulating function, which allows to represent the fluctuating response as a uniformly modulated random process.

The spectral moments of the fluctuating response, as well as the expected value of its maximum, are derived, based on an extension of the Davenport theory to nonstationary random processes. This is achieved assuming the maximum of the mean part of the response as the maximum static response to the mean part of the load, while the maximum of the fluctuating part is estimated employing equivalent parameters adapting a technique from the literature. Moreover, a correction following Der Kiureghian approach to mitigate the overestimations of the expected maximum value due to the Poisson approximation has been introduced.

The availability of a large database of thunderstorm records allows to check the reliability of the assumptions through a comparison between the analytical expression provided by the evolutionary thunderstorm model and those obtained numerically from the analysis of real events.

Results are compared in terms of mean value of the maximum response derived in time domain starting from real thunderstorm records. These comparisons show that on the one hand, the rigorous formulation offers a trustworthy method except for limited overestimations for very flexible and lowly damped structures, mainly due to the hypothesis of the contemporaneity of the maximum of the mean and fluctuating part of the response, along with the assumption of constant turbulent intensity inherent in the EPSD model of the wind velocity.

On the other hand, as previously discussed in literature, for stiffer and more damped structures it has been proved that the assumption of neglecting the dynamic effects of the modulating function is acceptable and consequently the hypothesis of simultaneous maxima of the mean and fluctuating part of the response is reliable. Hence, in these cases, the simplified formulation furnishes a handy and robust method for the prediction of the maximum dynamic response.

Future studies aim to investigate the reliability of identifying the maximum response with its mean value and to derive a closed-form solution for the EFRF and the equivalent parameters, in order to propose a handy tool for engineers dealing with the structural design. Moreover, since the modified Der Kiureghian method is based on the thunderstorm records available, the model may be tested to investigate the reliability of the method for thunderstorms from other regions of the world if new thunderstorms will be recorded. Finally, further studies aim to extend the approach to the dynamic analysis of MDOF systems.

CRediT authorship contribution statement

Luca Roncallo: Conceptualization, Methodology, Software, Validation, Formal analysis, Investigation, Data curation, Writing – original draft, Visualization. **Giovanni Solari:** Conceptualization, Methodology, Supervision, Project administration, Funding acquisition. **Giuseppe Muscolino:** Methodology, Supervision, Writing – review & editing. **Federica Tubino:** Supervision, Visualization, Writing – review & editing.

Declaration of competing interest

The authors declare that they have no known competing financial interests or personal relationships that could have appeared to influence the work reported in this paper.

Acknowledgements

This research is funded by the European Research Council (ERC) under the European Union's Horizon 2020 research and innovation program (grant agreement No. 741273) for the project THUNDERR - Detection, simulation, modelling and loading of thunderstorm outflows to design wind-safer and cost-efficient structures - supported by an Advanced Grant 2016.

The data used for this research was recorded by the monitoring network set up as part of the European Projects Winds and Ports (grant No. B87E09000000007) and Wind, Ports and Sea (grant No. B82F13000100005), funded by the European Territorial Cooperation Objective, Cross-border program Italy-France Maritime 2007–2013.

Appendix I

The geometrical spectral moments, also known as Vanmarcke's spectral moments, were introduced for the first time by Vanmarcke (1972) for stationary processes and are key quantities employed in the first passage problem for the assessment of structural failure. Their geometrical interpretation is related to the geometrical properties of the PSD of the process for which they offer a complete description.

Although there are no obstacles from a conceptual point of view to extend these quantities to the nonstationary case, this operation is not straightforward since the integral of the first and second moments may result unbounded (Corotis et al., 1972; Michaelov et al., 1999). This shortcoming was firstly solved by Di Paola (1985), who introduced the so-called "pre-envelope" process and defined as spectral characteristics its auto- and cross-covariances and its derivatives, while the definition of NGSMs is due to Michaelov et al. (1999). In this way the geometrical interpretation of these spectral characteristics is left behind replacing efficiently the role of the spectral moments in the case of a nonstationary random process.

Consider a zero-mean evolutionary process $r(t)$, representative of the loading conditions of a linear elastic SDOF system, characterized by the one-sided EPSD:

$$S_r(n,t) = |a(n,t)|^2 S_{r_0}(n) \tag{53}$$

where $a(n,t)$ is the deterministic complex-valued modulating function and $S_{r_0}(n)$ the one-sided PSD of the embedded stationary process. The one-sided EPSD of the dynamic response of the system, identified by its displacement $x(t)$, reads:

$$S_x(n,t) = |Z(n,t)|^2 S_{r_0}(n) \tag{54}$$

where the function $Z(n,t)$ is the evolutionary frequency response function (EFRF) and can be interpreted as the response of the SDOF system to the deterministic complex function $\varphi(n,t) = e^{i2\pi n\tau} a(n,\tau)$.

The EFRF and its derivative respect to time $\dot{Z}(n,t)$ are defined as follows:

$$Z(n,t) = \int_0^t h(t-\tau) e^{i2\pi n\tau} a(n,\tau) d\tau \tag{55}$$

$$\dot{Z}(n,t) = \int_0^t \dot{h}(t-\tau) e^{i2\pi n\tau} a(n,\tau) d\tau \tag{56}$$

where $h(t)$ is the impulse response of the system:

$$h(t) = \frac{1}{m\omega_d} e^{-\xi\omega_0 t} \sin(\omega_d t) \tag{57}$$

The NGSMs, namely $c_{jk,x}$, of the response read (Barbato and Conte, 2008, 2011; Michaelov et al., 2001):

$$c_{jk,x}(t) = (-1)^k i^{j+k} \int_0^{+\infty} S_{x^{(j)}x^{(k)}}(n,t) dn \tag{58}$$

where $j,k = 0,1,\ldots,N$ are the orders of the derivatives of x with respect to time and $S_{x^{(j)}x^{(k)}}$ the cross-EPSD of the processes $x^{(j)}$ and $x^{(k)}$. It was proved (Alderucci and Muscolino, 2017; Muscolino and Alderucci, 2015) that:

$$c_{00,x}(t) = \int_0^{+\infty} Z^*(n,t) Z(n,t) S_{r_0}(n) dn = \sigma_x^2(t) \tag{59}$$

$$c_{11,x}(t) = \int_0^{+\infty} \dot{Z}^*(n,t) \dot{Z}(n,t) S_{r_0}(n) dn = \sigma_{\dot{x}}{}^2(t) \tag{60}$$

where * denotes the complex conjugate. Hence, the variance of the displacement and velocities of the response, namely σ_x^2 and $\sigma_{\dot{x}}{}^2$, coincide with the NGSMs $c_{00,x}$ and $c_{11,x}$ respectively, which are real functions.

Accordingly, the expected frequency, the bandwidth parameter and the correlation coefficient can be defined as follows (Barbato and Conte, 2008, 2011, 2014; Michaelov et al., 1999, 2001):

$$\nu_x(t) = \frac{1}{2\pi} \sqrt{\frac{c_{11,x}(t)}{c_{00,x}(t)}} \tag{61}$$

$$q_x(t) = \sqrt{1 - \frac{\{Re[c_{01,x}(t)]\}^2}{c_{00,x}(t) c_{11,x}(t)}} \tag{62}$$

$$\rho_{x\dot{x}}(t) = -\frac{Im[c_{01,x}(t)]}{\sqrt{c_{00,x}(t) c_{11,x}(t)}} \tag{63}$$

It is worth to point out that the spectral characteristics in Eqs. (61)-(63) do not have geometrical interpretations, being derived from the NGSMs. However, they coincide with the geometric spectral moments when applied to a stationary process (Michaelov et al., 1999, 2001).

References

Abd-Elaal, E.-S., Mills, J.E., Ma, X., 2013. An analytical model for simulating steady state flows of downburst. J. Wind Eng. Ind. Aerod. 115, 53–64.

Alderucci, T., Muscolino, G., 2017. Time-frequency varying response functions of non-classically damped linear structures under fully non-stationary stochastic excitations. Probabilist. Eng. Mech. 54.

Barbato, M., Conte, J., 2014. Time-variant reliability analysis of linear elastic systems subjected to fully nonstationary stochastic excitations. J. Eng. Mech. 141, 4014173.

Barbato, M., Conte, J., 2011. Structural reliability applications of nonstationary spectral characteristics. J. Eng. Mech. 137, 371–382.

Barbato, M., Conte, J., 2008. Spectral characteristics of non-stationary random processes: theory and applications to linear structural models. Probabilist. Eng. Mech. 23, 416–426.

Burlando, M., Romanić, D., Solari, G., Hangan, H., Zhang, S., 2017. Field data analysis and weather scenario of a downburst event in Livorno, Italy, on 1 October 2012. Mon. Weather Rev. 145, 3507–3527.

Burlando, M., Zhang, S., Solari, G., 2018. Monitoring, cataloguing, and weather scenarios of thunderstorm outflows in the northern Mediterranean. Nat. Hazards Earth Syst. Sci. 18, 2309–2330.

Caracoglia, L., 2017. Parametric study on the use of the Fokker-Planck Equation to examine the nonstationary wind-induced dynamics of tall buildings. Procedia Eng 199, 3097–3102.

Chay, M., Albermani, F., 2005. Dynamic response of a SDOF system subjected to simulated downburst winds. Proc., Asia-Pacific Conf. Wind Eng.
Chay, M.T., Albermani, F., Wilson, R., 2006. Numerical and analytical simulation of downburst wind loads. Eng. Struct. 28, 240–254.
Chen, L., Letchford, C.W., 2005. Proper orthogonal decomposition of two vertical profiles of full-scale nonstationary downburst wind speeds. J. Wind Eng. Ind. Aerod. 93, 187–216.
Chen, L., Letchford, C.W., 2004a. A deterministic-stochastic hybrid model of downbursts and its impact on a cantilevered structure. Eng. Struct. 26, 619–629.
Chen, L., Letchford, C.W., 2004b. Parametric study on the along-wind response of the CAARC building to downbursts in the time domain. J. Wind Eng. Ind. Aerod. 92, 703–724.
Chen, X., 2008. Analysis of alongwind tall building response to transient nonstationary winds. J. Struct. Eng. 134, 782–791.
Choi, E.C., Hidayat, F.A., 2002. Dynamic response of structures to thunderstorm winds. Prog. Struct. Eng. Mater. 4, 408–416.
Corotis, R.B., Vanmarcke, E.H., Cornell, A.C., 1972. First passage of nonstationary random processes. J. Eng. Mech. Div.
Davenport, A.G., 1967. Gust loading factors. J. Struct. Div. 93, 11–34.
Davenport, A.G., 1964. Note on the distribution of the largest value of a random function with application to gust loading. Proc. Inst. Civ. Eng. 28, 187–196.
Davenport, A.G., 1961. The application of statistical concepts to the wind loading of structures. ICE Proc 19, 449–472.
De Gaetano, P., Repetto, M.P., Repetto, T., Solari, G., 2014. Separation and classification of extreme wind events from anemometric records. J. Wind Eng. Ind. Aerod. 126, 132–143.
Der Kiureghian, A., 1980. Structural response to stationary excitation. J. Eng. Mech. Div. 106, 1195–1213.
Di Paola, M., 1985. Transient spectral moments of linear systems. SM Arch 10, 225–243.
Holmes, J., Forristall, G., Mcconochie, J., 2005. Dynamic response of structures to thunderstorm winds. In: 10th Americas Conference on Wind Engineering, ACWE 2005.
Holmes, J.D., Hangan, H.M., Schroeder, J.L., Letchford, C.W., Orwig, K.D., 2008. A forensic study of the Lubbock-Reese downdraft of 2002. Wind Struct. An Int. J. 11, 137–152.
Hu, L., Xu, Y.L., 2014. Extreme value of typhoon-induced non-stationary buffeting response of long-span bridges. Probabilist. Eng. Mech. 36, 19–27.
Huang, G., Chen, X., 2009. Wavelets-based estimation of multivariate evolutionary spectra and its application to nonstationary downburst winds. Eng. Struct. 31, 976–989.
Huang, G., Chen, X., Liao, H., Li, M., 2013. Predicting of tall building response to non-stationary winds using multiple wind speed samples. Wind Struct. An Int. J. 17, 227–244.
Huang, G., Zheng, H., Xu, Y.-L., Li, Y., 2015. Spectrum models for nonstationary extreme winds. J. Struct. Eng. (United States) 141.
Kareem, A., Hu, L., Guo, Y., Kwon, D.-K., 2019. Generalized wind loading chain: time-frequency modeling framework for nonstationary wind effects on structures. J. Struct. Eng. (United States) 145.
Kwon, D.K., Kareem, A., 2019. Towards codification of thunderstorm/downburst using gust front factor: model-based and data-driven perspectives. Eng. Struct. 199, 109608.
Kwon, D.K., Kareem, A., 2013. Generalized gust-front factor: a computational framework for wind load effects. Eng. Struct. 48, 635–644.
Kwon, D.K., Kareem, A., 2009. Gust-front factor: a new framework for wind load effects on structures. J. Struct. Eng. 135, 717–732.
Le, T.-H., Caracoglia, L., 2017. Computer-based model for the transient dynamics of a tall building during digitally simulated Andrews AFB thunderstorm. Comput. Struct. 193, 44–72.
Le, T.-H., Caracoglia, L., 2015. Wavelet-Galerkin analysis to study the coupled dynamic response of a tall building against transient wind loads. Eng. Struct. 100, 763–778.
Lin, Y.K., Cai, G.Q., 1995. Probabilistic Structural Dynamics : Advanced Theory and Applications, Probabilistic Structural Dynamics Advanced Theory and Applications. McGraw-Hill, New York.
Lombardo, F.T., Smith, D.A., Schroeder, J.L., Mehta, K.C., 2014. Thunderstorm characteristics of importance to wind engineering. J. Wind Eng. Ind. Aerod. 125, 121–132.
Lombardo, F.T., Zickar, A.S., 2019. Characteristics of measured extreme thunderstorm near-surface wind gusts in the United States. J. Wind Eng. Ind. Aerod. 193, 103961.
McConville, A.C., Sterling, M., Baker, C.J., 2009. The physical simulation of thunderstorm downbursts using an impinging jet. Wind Struct 12.
Michaelov, G., Lutes, L.D., Sarkani, S., 2001. Extreme value of response to nonstationary excitation. J. Eng. Mech. 127, 352–363.
Michaelov, G., Sarkani, S., Lutes, L.D., 1999. Spectral characteristics of nonstationary random processes — a critical review. Struct. Saf. 21, 223–244.
Muscolino, G., 2012. Dinamica delle strutture: con fondamenti ed applicazioni di ingegneria sismica e dinamica aleatoria. Pitagora Editrice, Bologna.
Muscolino, G., Alderucci, T., 2015. Closed-form solutions for the evolutionary frequency response function of linear systems subjected to separable or non-separable non-stationary stochastic excitations. Probabilist. Eng. Mech. 40, 75–89.
Peng, L., Huang, G., Chen, X., Yang, Q., 2018. Evolutionary spectra-based time-varying coherence function and application in structural response analysis to downburst winds. J. Struct. Eng. 144, 1–16.
Piccardo, G., Poggi, S., Solari, G., 2018. Some critical issues on the distribution of the maximum value of the wind-excited response of structures. Probabilist. Eng. Mech. 54, 65–81.
Ponte, J., Riera, J.D., 2010. Simulation of extreme wind series caused by thunderstorms in temperate latitudes. Struct. Saf. 32, 231–237.
Priestley, M.B., 1965. Evolutionary spectra and non-stationary processes. J. R. Stat. Soc. Ser. B 27, 204–237.
Repetto, M.P., Burlando, M., Solari, G., De Gaetano, P., Pizzo, M., 2017. Integrated tools for improving the resilience of seaports under extreme wind events. Sustain. Cities Soc. 32, 277–294.
Repetto, M.P., Burlando, M., Solari, G., De Gaetano, P., Pizzo, M., Tizzi, M., 2018. A web-based GIS platform for the safe management and risk assessment of complex structural and infrastructural systems exposed to wind. Adv. Eng. Software 117, 29–45.
Roncallo, L., Solari, G., 2020. An evolutionary power spectral density model of thunderstorm outflows consistent with real-scale time-history records. J. Wind Eng. Ind. Aerod. 203.
Roncallo, L., Solari, G., 2019. Modelling of thunderstorm outflows by means of the evolutionary power spectral density. In: 15th International Conference on Wind Engineering (ICWE 15). Beijing, China.
Solari, G., 2019. Wind Science and Engineering: Origins, Developments, Fundamentals and Advancements. Springer Science and Business Media LLC.
Solari, G., 2016. Thunderstorm response spectrum technique: theory and applications. Eng. Struct. 108, 28–46.
Solari, G., 1993a. Gust buffeting .1. Peak wind velocity and equivalent pressure. J. Struct. Eng. 119, 365–382.
Solari, G., 1993b. Gust buffeting .2. Dynamic alongwind response. J. Struct. Eng. 119, 383–398.
Solari, G., 1988. Equivalent wind spectrum technique: theory and applications. J. Struct. Eng. 114, 1303–1323.
Solari, G., 1982. Alongwind response estimation: closed form solution. J. Struct. Div. 108, 225–244.
Solari, G., Burlando, M., De Gaetano, P., Repetto, M.P., 2015a. Characteristics of thunderstorms relevant to the wind loading of structures. Wind Struct. An Int. J. 20, 763–791.
Solari, G., De Gaetano, P., 2018. Dynamic response of structures to thunderstorm outflows: response spectrum technique vs time-domain analysis. Eng. Struct. 176, 188–207.
Solari, G., De Gaetano, P., Repetto, M.P., 2015b. Thunderstorm response spectrum: fundamentals and case study. J. Wind Eng. Ind. Aerod. 143, 62–77.
Solari, G., Piccardo, G., 2001. Probabilistic 3-D turbulence modeling for gust buffeting of structures. Probabilist. Eng. Mech. 16, 73–86.
Solari, G., Rainisio, D., De Gaetano, P., 2017. Hybrid simulation of thunderstorm outflows and wind-excited response of structures. Meccanica 52, 3197–3220.
Solari, G., Repetto, M.P., Burlando, M., De Gaetano, P., Pizzo, M., Tizzi, M., Parodi, M., 2012. The wind forecast for safety management of port areas. J. Wind Eng. Ind. Aerod. 104–106, 266–277.
Tubino, F., Solari, G., 2020. Time varying mean extraction for stationary and nonstationary winds. J. Wind Eng. Ind. Aerod. 203, 104187.
Vanmarcke, E.H., 1972. Properties of spectral moments with applications to random vibration. J. Eng. Mech. Div. 98, 425–446.
Zhang, S., Solari, G., Burlando, M., Yang, Q., 2019. Directional decomposition and properties of thunderstorm outflows. J. Wind Eng. Ind. Aerod. 189, 71–90.
Zhang, S., Solari, G., De Gaetano, P., Burlando, M., Repetto, M.P., 2017. A refined analysis of thunderstorm outflow characteristics relevant to the wind loading of structures. Probabilist. Eng. Mech.
Zhang, S., Solari, G., Yang, Q., Repetto, M.P., 2018. Extreme wind speed distribution in a mixed wind climate. J. Wind Eng. Ind. Aerod. 176, 239–253.